Journal Pre-proof

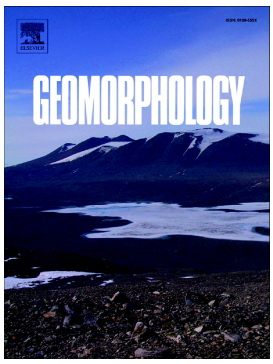

Spatial organisation and physical characteristics of large peat blocks in an upland fluvial peatland ecosystem

Richard J. Boothroyd, Jeff Warburton

PII: S0169-555X(20)30370-6

DOI: https://doi.org/10.1016/j.geomorph.2020.107397

Reference: GEOMOR 107397

To appear in: *Geomorphology*

Received date: 25 March 2020

Revised date: 21 August 2020

Accepted date: 21 August 2020

Please cite this article as: R.J. Boothroyd and J. Warburton, Spatial organisation and physical characteristics of large peat blocks in an upland fluvial peatland ecosystem, *Geomorphology* (2020), https://doi.org/10.1016/j.geomorph.2020.107397

Spatial organisation and physical characteristics of large peat blocks in an upland fluvial peatland ecosystem

Authors and Affiliations

Richard J. Boothroyd[1,2] and Jeff Warburton[2]

[1] School of Geographical and Earth Sciences, University of Glasgow, G12 8QQ, UK.

[2] Department of Geography, Durham University, Durham, DH1 3LE, UK.

E-mail: richard.boothroyd@glasgow.ac.uk

Abstract

This paper assesses the size, shape and spatial organisation of organic, carbon-rich debris (peat blocks) in an upland fluvial peatland ecosystem. Peat block inventories collected in 2002 and 2012 at an alluvial reach of Trout Beck (North Pennines; United Kingdom) provide independent surveys for investigating the physical characteristics and spatial organisation of the organic debris. Peat blocks deposited along the 450 m reach represent a substantial volume of fluvially derived in-channel sediment and carbon flux at the macroscale (total peat volume 11 m^3 (2002) and 17 m^3 (2012)). Results show that inferred peat block transport distances depend on their size and shape. Smaller and more spherical equant shaped peat blocks are transported 1.62 and 1.72 times the distance of prolate and elongate shaped peat blocks. Downstream fining relationships provide a first-order approximation of peat block degradation rates. These degradation rates are high (up to 2 mm/m for the a-axis) and indicate considerable fine sediment release during transport. Hypsometric relations show that 73% of peat blocks are distributed within 1 channel width of the thalweg, indicating lateral organisation and a pattern of preferential deposition at the active channel margin. The local effects of obstructions from topography, roughness and slope promote peat block deposition, but given the low density of the blocks and close proximity to the flow the potential for re-entrainment is high.

Key words

peat; degradation; sediment dynamics; carbon flux; abrasion; deposition

1. Introduction

Fluvial erosion is an important process governing the short- and long-term evolution of peatland ecosystems and can produce significant fluxes of organic carbon (Evans *et al.*, 2006). The delivery of peat from degraded peatlands provides an indicator of the erosional status and is crucial in quantifying carbon balances (Evans and Warburton, 2007). Peat transported in river channels is typically in the form of fine suspended sediment and larger, low-density (~1050 kg m^3) peat blocks that are sometimes referred to as organic debris (Evans and Warburton, 2001; Evans and Warburton, 2007; Warburton and Evans, 2011). Peat blocks have a range of physical characteristics, often with maximum orthogonal axis dimensions on the order of centimetres to metres (Evans and Warburton, 2007). They are typically classified according to their sedimentary setting and depositional form (Warburton and Evans, 2011). The implications of the processes acting on peat blocks are potentially large, given that peatlands dissected by fluvial erosion include most of the terrestrial peat store (~3 million km^2) and contain about 30 percent of all land-based carbon (550 GT) (IPCC, 2018). Although previous research on peat blocks has focussed on relatively steeply sloping blanket peatlands in the United Kingdom (Evans and Warburton, 2010), peat blocks are potentially widespread throughout various fluvially-dissected peatlands in different environmental settings (Figure 1); including sites of river bank failure in continuous permafrost settings (Walker et al., 1987). A key aim of this paper is to demonstrate the potential rapid breakdown of peat blocks by fluvial erosion and promote awareness of this phenomena to a wider audience.

Fluvial sediment budgets in peatlands can become dominated by the delivery of peat from sources lateral to the channel network (Evans and Warburton, 2005; Evans *et al.*, 2006). Sediment is frequently delivered as peat blocks through cantilever bank failure of fluvially undercut blanket peat at discrete sources and more intermittently through the delivery of peat rafts via mass failure events (Dykes and Warburton, 2007). More substantial volumes of peat can be delivered to the channel network by mass failure events. Following the complex of peat slides that impacted Channerwick (South Shetland; United Kingdom) on the 19th September 2003, it is estimated that ~100,000 m^3 of peat entered the channel network (Dykes and Warburton, 2008). A hiatus can occur between the

delivery of peat blocks to the fluvial system and their subsequent entrainment and transmission (Evans and Warburton, 2001), while catchment storage processes can reduce the efficiency of sediment delivery to the downstream fluvial system and interrupt catchment export (Walling, 1983).

Once entrained, peat block transport depends on the critical submergence depth (block size, B_s, relative to flow depth, d) with three transport phases identified: flotation, saltation and rolling (Figure 2) (Evans and Warburton, 2001). Transition between transport phases primarily occurs as a function of a fining peat block size or varying flow depth. During transport, the rate of degradation is linked to contact with the bed, with the rolling phase responsible for greatest losses as peat blocks split, break and abrade. Stalling/lodging can occur when the flow depth is approximately half the peat block size or less (Evans and Warburton, 2001), resulting in deposition across the active channel margin (e.g. Figure 1c). Following deposition, peat block residence times are variable and depend on whether the block is re-entrained or becomes buried in the floodplain stratigraphy. Warburton and Evans (2011) quantified an average residence time of 168 days for re-entrained blocks, compared to an average of 617 days for blocks that were eventually incorporated into the floodplain stratigraphic sequence. The spatial organisation of deposited peat blocks has implications for the proportion of peat blocks that are exported out of the fluvial system, and the proportion that are locked away in the floodplain stratigraphy (Warburton and Evans, 2011).

Peat blocks are not usually included in carbon balance estimates of blanket peatlands dissected by fluvial erosion (Evans and Warburton, 2007). This is potentially significant because the carbon content of ombrotrophic blanket mire peat typically ranges between 50-53% dry weight (Lindsay, 2010). Fluvial carbon export primarily occurs as particulate and dissolved organic carbon (POC and DOC) and dissolved CO_2 (Worrall et al., 2009). POC has been shown to undergo transformation to DOC or become mineralized to CO_2 during periods of floodplain storage (Pawson, 2008; Pawson et al., 2012; Moody et al., 2013). Evans and Warburton (2007) introduce the term 'block' organic carbon (BOC) to refer to peat blocks in organic carbon cascades, but the magnitude of flux between the carbon pathways, and the contribution and significance of peat blocks to the organic carbon cascade, remain relatively unknown. Where atmospheric interactions heighten CO_2 release through

oxidation (Pawson *et al.*, 2012), incorporation of peat blocks into the floodplain stratigraphy allows carbon sequestration (Evans and Lindsay 2010; Warburton and Evans, 2011). Floodplains have been described as both hotspots for carbon cycling and as areas of sequestration in upland fluvial peatland ecosystems (Alderson *et al.*, 2019). An improved process-understanding of peat block transfer, degradation and residence through fluvial systems is essential for establishing representative carbon budgets (Evans and Warburton, 2007).

Ecologically, peat blocks represent a macroscale roughness element that impart flow heterogeneity to the channel (Crowe and Warburton, 2007). This produces a spatial patchiness in flow field dynamics and contributes towards the unequal provision of turbulence, a key abiotic factor in microhabitat provision (Davis and Barmuta, 1989). Peat blocks contribute towards the areas of channels capable to act as refugia, provide food resources and remove waste, all of which are required for the consistent functioning of invertebrate and macroinvertebrate ecosystems (Townsend, 1989; Bouckaert and Davis, 1998; Beisel *et al.*, 2000; Passy, 2001). Fine sediment is eroded from the sides of deposited peat blocks (Crowe and Warburton, 2007) where organic sediment is a key control on invertebrate ecosystem dynamics (Rice et al., 2001) and fine particulate organic sediment accumulations are associated with significant changes in macroinvertebrate biodiversity (Ramchunder et al., 2012). Short pulses of organic sediment have a negative association with the benthos and macroinvertebrate community composition (Aspray et al., 2017) and sedimentation can alter headwater invertebrate biodiversity, decreasing the density and richness at the community level (Brown et al., 2019). Fine sediment release from peat blocks has a range of ecological significances.

Here, we aim to improve the understanding of the physical characteristics and spatial organisation of peat blocks in an upland peatland ecosystem dissected by fluvial erosion. By constraining the quantity and distribution of peat blocks, we will contribute towards better understanding the geomorphic, carbon and ecological functioning of the peatland riverscape. This will be achieved by comparing two temporally independent peat block inventories collected in 2002 and 2012 and linking these to a high-resolution topographic dataset. The independence of the two inventories, spaced 10 years apart, can be justified based on the high turnover of peat blocks within the active fluvial system

(Warburton and Evans, 2011) and the contrasting weathered form of long-term stored peat blocks cf. freshly delivered blocks. Physical characteristics (i.e. size and shape) will be related to their hypsometric distribution to better understand the spatial patterns and gradients of peat blocks across the riverscape. Results will improve our understanding of the extent and distribution of carbon-rich debris in an actively eroding peatland ecosystem, relevant for catchment sediment and carbon budgets. The paper considerably differs from previous work by Evans and Warburton (2001) that focussed on mechanisms and patterns of peat block transfer; and Warburton and Evans (2011) that concentrated on sedimentation implications around deposited blocks. The main objectives are threefold, to:

1) Produce spatially referenced inventories for peat block size and shape from repeat surveys.
2) Compare physical characteristics between temporally independent inventories, to determine the coherence and persistence of peat block characteristics.
3) Understand the spatial organisation of peat block distributions with respect to:
    i). Inferred distance downstream from discrete peat sources (for first-order approximations of peat block degradation rates and fine sediment release).
    ii). Vertical and lateral organisation relative to the channel thalweg using hypsometric relations (to assess depositional patterns and processes).

2. Materials and Methods

2.1 Study site

Field data were collected along a 450 m reach of an upland peatland channel in the Trout Beck catchment (11.4 km^2), situated in the Moor House National Nature Reserve (North Pennines; United Kingdom) (Figure 3a). Across the catchment it is estimated that 17% of the peat blanket has been actively eroded (Garnett and Adamson, 1997), with dendritic type I gullying producing wandering channels on lower gradient slopes and linear type II gullying aligned normal to the slope on steeper gradients (Bower 1961). The peat type is dominated by *Eriophorum* sp, *Calluna vulgaris* and *Sphagnum* sp and has been accumulating for approximately 7500 years since the late Boreal (Conway,

1954). Blanket peat covers ~90% of the catchment, with the depth averaging 1-3 m (Holden and Burt, 2003). Blanket peat overlies the dominant surficial geology of reworked periglacial tills and fluvially derived overbank deposits (Aitkenhead *et al.,* 2002). The bedrock geology is of the Carboniferous sequence, consisting of almost horizontally interbedded limestones, sandstones and shales (Johnson and Dunham, 1963).

Multiple lower order surficial peatland streams combine to form the higher order Trout Beck channel, a tributary of the River Tees (Figure 3a). The channel bed is composed of poorly sorted cobble sized clasts, where the D_{50} value ranges from 8-80 mm (Crowe and Warburton, 2007). The bedrock outcrops in the Trout Beck channel produce an alternating sequence of alluvial and bedrock reaches (Ferguson *et al.,* 2017). The selected alluvial study reach (Figure 3b) has an elevation of ~540 m, is characterised by an average slope of 0.015, and has an average wetted width of approximately 10 m. The channel is surrounded by a narrow fragmentary floodplain which in part is laterally confined by steep banks. Discharge is monitored at a downstream compound Crump weir, maintained by the Environment Agency (EA) as part of the Environmental Change Network (ID 25003). In the period of record 1957-2018 (81% completeness), mean daily flow was 0.56 m^3/s, 10% exceedance (Q10) was 1.56 m^3/s and 5% exceedance (Q5) was 2.30 m^3/s (NRFA, 2020).

Three discrete peat sources where cantilever failure of the blanket peat was observed were identified and mapped (Figure 3b). Peat sources were identified in the field by looking at the degree of undercutting, steepness of banks, presence of failed peat blocks and disturbance of vegetation (Evans and Warburton, 2005). The study site represents an actively eroding alluvial reach of Trout Beck, so peat block release is likely to be higher than in nearby semi-alluvial and bedrock reaches, where the potential for bank erosion is reduced. However, similar actively eroding alluvial reaches are observed further upstream and in neighbouring catchments (e.g. River Tees), so the study site is representative of the wider behaviour of the upland fluvially-dissected peatland ecosystem.

2.2 Peat block inventories

We collected field data on multiple site visits in October 2012. The contemporary inventory was

spatially referenced using a Garmin eTrex H GPS unit, mapping the location of peat blocks, peat sources and the channel thalweg with a typical horizontal accuracy of < 1 m. For each of the mapped peat blocks, three orthogonal axis length measurements were recorded (a-, b- and c-axis; ± 0.01 m error). Only peat blocks with an a-axis length greater than 0.1 m were sampled (n = 127). A comparable inventory, using identical survey methods, was collected along the same study reach in February 2002 (n = 123); except a Magellan GPS ProMARK X CP was used for spatial referencing. The decadal interval between repeat surveys allows for the general governing physical processes to be tested. A first-order approximation of peat block volume was made by assuming a cubic shape and multiplying orthogonal axis lengths (a-axis * b-axis * c-axis). Peat block shape was classified by plotting the ratio of b-axis/a-axis against c-axis/b-axis to produce a Zingg-type diagram, with shape classified as elongate, equant, prolate or tabular. Classifying peat blocks using orthogonal axis dimensions has the additional benefit of relating directly to the characteristic mechanics of block transport (e.g. rolling, saltating, etc) (Evans and Warburton, 2001). Peat block morphology is represented by the Corey shape index (sphericity, 0-1) and disk-rod index (disk-rodness, 0-1) (Sneed and Folk, 1958; Illenberger, 1991). From the nearby gauging station, peak daily flow for the 12 months preceding the 2002 inventory was 4.88 m^3/s (event occurred 18 days before the inventory; annual record 77% complete) and 11.7 m^3/s in 2012 (event occurred 115 days before the inventory; annual record 100% complete).

2.3 Digital Elevation Model (DEM)

A Leica Geosystems Real Time Kinetic differential GPS 1200 (RTK dGPS) was used to survey channel and floodplain topography in April 2012. Elevation measurements were recorded at 28671 discrete points and interpolated to produce a digital elevation model (DEM) with a spatial resolution of 0.5 m. The DEM was used for the topographic analysis of the peat block inventory, with the area of DEM data coverage shown in Figure 3b.

2.4 Inferred transport distances and the spatial organisation of deposited peat blocks

We used the mapped peat block positions and the DEM to undertake spatial and topographic analyses.

We inferred peat block transport distances by measuring the Euclidean distance from the upstream edge of peat sources to individual peat blocks. Transport was assumed to initiate from the nearest peat source, with transport only possible in the downstream direction. Rationale for this assumption is based on the presence of semi-alluvial and bedrock reaches immediately upstream of the study reach (Ferguson *et al.,* 2017). For peat blocks transported through the semi-alluvial and bedrock reaches, mechanical breakdown is assumed to be high from channel bed and sidewall contact along a 0.3 km long bedrock gorge with topographic irregularities that have a sidewall roughness length on the order of several decimetres (Ferguson *et al.,* 2019). In addition, the size and morphology of the peat blocks, stored in a given reach, is often diagnostic of locally-sourced versus far-travelled blocks i.e. far-travelled peat blocks are much smaller and have far greater rounding than locally-sourced material.

Furthermore, we quantified the vertical and lateral organisation of peat blocks relative to the mapped channel thalweg. Hypsometric relations were investigated by plotting peat block frequency and volume against: (i) vertical height above; and (ii) lateral distance away from the channel thalweg. The channel thalweg provides a temporally consistent reference point from which vertical and lateral distances were calculated. The spatial organisation of peat blocks relative to (i) and (ii) were normalised between values of 0 and 1 to compare vertical and lateral peat block distributions. These data provide hypsometric relations, allowing for the identification of zones where peat block distribution is relatively abundant or sparse.

3. Results

3.1 Spatial distribution of peat blocks

Peat blocks are deposited in several clusters in the 2012 inventory (Figure 4). This tendency for clustering was previously demonstrated across a range of environmental settings (Figure 1) and suggests that it is unusual for peat blocks to be deposited in isolation. Peat blocks tend not to be deposited within the active region of the channel, instead deposition is favoured at the margins of the channel on mid-channel bars, or overbank on floodplain pockets proximal to channel bends. Similar spatial distributions are repeated in other reaches in the catchment. Furthermore, peat blocks are

rarely located close to the sources of cantilever bank failure. For the few peat blocks that do appear immediately downstream (< 10 m) from source zones (3% in 2002; 2% in 2012), it is assumed that these peat blocks have recently failed and are yet to be entrained by high flows. This indicates dispersion of peat blocks, supporting the argument for peat blocks being efficiently transferred through the fluvial system (Evans and Warburton, 2001).

3.2 Peat block size and classified shape

There is considerable variation in the size of peat blocks in the 2002 and 2012 inventories (Figure 5; Table 1). A range of values are recorded across peat block orthogonal axes, with the range in a-axis exceeding 2 m and the range in b-axis exceeding 1 m. Standard deviations are equivalent to approximately 50% of the mean axis lengths, indicating substantial variation in orthogonal axis dimensions. Peat block dimensions vary and this is temporally consistent between the inventories (Figure 5). The data on orthogonal axes are non-normally distributed; positive skewness values, particularly for a-axis and volume, indicate there are few extremely large values. The positive kurtosis values, particularly for volume, indicate the data are heavily tailed (Figure 5). Due to the marked variation in peat block size, it is difficult to generalise peat block dimensions to a characteristic value. Instead, peat block dimensions are reported to be on the order of centimetres to metres. Comparing the total estimated volume of peat blocks, the inventory from 2012 (16.68 m^3) is 58.9% larger than the inventory in 2002 (10.50 m^3). This represents a considerable volume of both sediment and carbon flux at the macroscale.

In terms of shape, the mean a-axis typically exceeds the mean b-axis by approximately 1.5-2, suggesting that characteristic peat block shape is non-cubic. Peat block shape is classified by plotting the ratio of b-axis/a-axis against c-axis/b-axis to produce a Zingg-type diagram (Figure 6). Elongate shapes are most abundant in the 2002 inventory (46%), followed by prolate (27%), tabular (22%) and equant (5%). In the 2012 inventory, equant shapes are most abundant (42%), followed by tabular (22%), prolate (20%) and elongate (16%). The sparsity of equant peat blocks in the 2002 inventory is notable and demonstrates that the proportions of classified shapes has changed through time,

indicating temporal incoherence in classified shape.

The relationships between peat block size (b-axis and volume) and classified shape are shown in Figure 7 and Table 2. For equant, elongate and prolate shaped peat blocks, the differences in b-axis and volume are not statistically significant between the 2002 and 2012 inventories (Mann-Whitney test, *p*-value > 0.001). For tabular shaped peat blocks, the differences in b-axis and volume are statistically significant between 2002 and 2012 (Mann-Whitney test, *p*-value < 0.001). When classified by shape, the size of most peat blocks has remained the same through time, indicating temporal coherence in peat block size. Where the 2002 and 2012 inventories are combined, differences in b-axis and volume are not statistically significant between peat blocks of different classified shape (Kruskal Wallis test, b-axis: *p*-value > 0.001; volume: *p*-value > 0.001). Overall, peat blocks with different classified shapes are not significantly different in size.

3.3 Inferred peat block transport distances

The mean inferred transport distance has almost doubled from 64.07 m in 2002 to 120.79 m in 2012 (Table 1). Peat block transport distances are greater in the 2012 inventory and this difference is statistically significant (Mann-Whitney test, *p*-value < 0.001). A summary of the changes in peat block size, morphology and inferred transport distance for the classified shapes are shown in Table 2. Statistically significant differences in the inferred transport distance between peat blocks of different classified shape are noted (Kruskal Wallis test, *p*-value < 0.001). Equant shaped blocks are transported the greatest mean distance (125.60 m), have the smallest peat block size and were most spherical (mean Corey shape index of 0.73). Evans and Warburton (2007) had previously suggested a positive feedback whereby smaller peat blocks are transported greater distances. Tabular shaped blocks are transported a mean distance of 101.78 m, have a comparably small mean volume (0.08 m^3), but differed from equant shaped blocks in terms of a lower sphericity and more disk-like morphology (mean disk-rod index of 0.32). Shorter mean transport distances are shown for prolate (77.59 m) and elongate (73.23 m) shaped blocks. Prolate shaped blocks have a larger mean block volume (0.18 m^3) and more rod-like morphology (mean disk-rod index 0.84); whereas elongate shaped blocks have the

lowest overall block sphericity (mean Corey shape index of 0.36). Therefore, equant shaped peat blocks are transported 1.62 and 1.72 times the distance of prolate and elongate shaped peat blocks, and this difference is statistically significant (Mann-Whitney tests, p-value < 0.001).

3.4 First-order approximations of peat block degradation rates

Downstream fining relationships are shown in Figure 8, with considerable scatter an artefact of the clustering and spatial organisation of deposited peat blocks (e.g. 150-200 m downstream). Inferred peat block transport distances for the 2002, 2012 and combined inventories are regressed against orthogonal axes (Figure 8a-c). First-order approximations of peat block degradation rates are estimated by fitting a linear regression to block axes and the inferred transport distance. The statistical relationship between a-axis and transport distance is characterised by a low coefficient of determination ($R^2 = 0.097$), but a statistically significant negative slope ($\alpha = -0.00245$ and p-value < 0.001). The slope of the regression corresponds to a peat a-axis degradation rate of 2.45 mm/m (n = 250). Caution is noted when using this approach; the low coefficient of determination indicates that only a small fraction of the variance is explained by the parameters, and there is considerable scatter in downstream fining sequences. Regressions for the b-axis and c-axis are not presented because the coefficient of determinations were lower, and the slopes not statistically significant. By applying the same process to a sample of b-axis peat block measurements collected at Trout Beck in 1997 published in Evans and Warburton (2007), a similar order of magnitude in peat block degradation rate is quantified (4.18 mm/m; n = 61). Although these estimates provide only a first-order approximation of peat block degradation rates, they indicate the rapid breakdown of transported peat blocks; consistent with measurements of specific abrasion rates from field experiments on small peat blocks (Evans and Warburton, 2001).

Peat block degradation rates are used to estimate fine sediment release (Table 3). From the inferred transport distance of each peat block, a characteristic range of peat block degradation rates are applied to back-calculate initial peat block volumes (i.e. pre-transport) and estimate the potential volume of fine sediment release. Degradation rate scenarios are designed to represent the first-order degradation

rates quantified here, and illustrate both equal (a-axis = b-axis = c-axis) and unequal (a-axis > b-axis > c-axis) degradation losses across peat block orthogonal axes. Were the peat block degradation rates an order of magnitude lower than those estimated here (i.e. DR1, 0.5 mm/m a-, b- and c-axis), 1.66 m^3 of fine sediment would have been released in the 2002 inventory and 5.34 m^3 in the 2012 inventory. This fine sediment release would represent 14 and 24% of the pre-transport peat block volume. Were the peat block degradation rates comparable to those estimated here (i.e. DR3, 2 mm/m a-, b- and c-axis), substantially greater volumes of fine sediment would have been released (2002 = 9.64 m^3 or 48% of the pre-transport peat block volume; 2012 = 32.08 m^3 or 66% of pre-transport peat block volume). Were peat block losses only recorded across the a-axis (i.e. DR5, 2 mm/m a-axis, no losses b- and c-axis), then volumes of fine sediment release are smaller (2002 = 0.96 m^3 or 8% of the pre-transport peat block volume; 2012 = 3.86 m^3 or 19% of pre-transport peat block volume). Finally, if peat block degradation rates were comparable to those estimated here, but unequal across orthogonal axes (i.e. DR6, 2 mm/m a-axis, 1 mm/m b-axis and 0.5 mm/m c-axis), then considerable volumes of fine sediment would be released (2002 = 3.34 m^3 or 24% of the pre-transport peat block volume; 2012 = 11.99 m^3 or 42% of the pre-transport peat block volume). Scenario testing reveals the potentially large volumes of fine sediment released from inventoried peat blocks during transport (mean average of DR1-DR7 estimates in 2002 = 8.57 m^3; 2012 = 28.54 m^3).

3.5 Spatial organisation of deposited peat blocks

To better understand the spatial organisation of deposited peat blocks from the 2012 inventory, normalised vertical heights and lateral distances from the channel thalweg are mapped (Figure 9) and the abundance quantitatively assessed using hypsometric relations (Figure 10). All mapped peat blocks lie within a tight vertical height range from the channel thalweg (0-0.71 m); whereas the range of lateral distances is wider (0-21.08 m). For hypsometric relations, divergence from $x = y$ indicates either an abundance (flatter sections) or sparseness (steeper sections) of deposited peat blocks.

The vertical organisation (Figure 9a) shows that spatial clusters of peat blocks have similar normalised heights above the channel thalweg (e.g. the group of peat blocks perched on the mid-

channel bar are associated with similar heights above the channel thalweg). Hypsometric relations (Figure 10a) show that peat blocks are almost uniformly distributed with height above the channel thalweg, with only minor deviations from the line of equality. The associated histogram shows that 28% of peat blocks are distributed in the lower third of the normalised profile, 44% in the middle third, and 28% in the upper third. This suggests that peat block deposition is almost equally likely over the range of mapped heights. The tight range of heights and uniform vertical distribution above the channel thalweg suggest that peat blocks are transported close to the maximum stage of flood flows. Peat block deposition through stalling is sensitive to the small changes in the hydraulic surface (Figure 2), and this sensitivity is recorded in the spatial organisation of deposited peat blocks.

The lateral organisation of peat blocks (Figure 9b) demonstrates preferential deposition proximal to the channel thalweg. Peat block transport is therefore aligned to the channel thalweg. Hypsometric relations (Figure 10b) show a more marked deviation from the line of equality, with an abundance of peat blocks at normalised lateral distances in the range 0.2-0.5. The zone where relatively more peat blocks are deposited extends approximately 1 channel width (up to ~10.5 m) from the channel thalweg. The associated histogram shows that 73% of peat blocks are distributed within 1 channel width of the thalweg, and that many of the largest peat blocks by volume are deposited here. A relatively sparse zone is shown at normalised distances > 0.75 (towards 2 channel widths from the channel thalweg), so fewer peat blocks are deposited beyond the active channel margin. The pronounced lateral organisation, with preferential deposition proximal to the active channel margin, suggest that peat blocks tend to be transported close to the channel thalweg (i.e. approximately within the confines of the active channel) and that deposition is associated with local obstructions from topography, roughness and changes in slope at the active channel margin.

For each peat block, normalised vertical and lateral positions are shown in Figure 11. For peat blocks deposited in or around the active channel margin, the normalised height above the thalweg increases with normalised distance from the channel thalweg, with most of the volumetrically largest peat blocks deposited in this zone. The relationship is indicative of rapid deposition associated with small changes in hydraulic surface. Beyond the active channel margin relatively few peat blocks are

deposited over a smaller range of heights. The hypsometric relations observed at Trout Beck suggest an underlying spatial organisation on peat block deposition; transport is aligned to the channel thalweg and small changes in the hydraulic surface and/or local obstructions from topography, roughness and slope promote peat block deposition at the active channel margin.

4. Discussion

Through the analysis of two temporally independent inventories collected in 2002 and 2012, peat blocks are characterised as having principal axes on the order of centimetres to metres, showing variation in their size and shape. Locally, individual peat blocks can represent large depositional features (maximum measured a-axis: 3.05 m; maximum estimated volume: 1.59 m^3). Large peat blocks have geomorphological and ecological significance, locally modifying the flow, controlling the deposition of gravel and even influencing channel planform (Evans and Warburton, 2007). The proportion of classified peat block shapes has changed through time; elongate shaped peat blocks were most abundant in 2002, whereas equant shaped peat blocks were most abundant in 2012 (Figure 6). Between classified peat block shapes, no statistically significant difference in peat block size was observed. Although most classified peat block shapes remained approximately the same size between inventories (Figure 7); only tabular shaped blocks showed a statistically significant difference in b-axis and volume. Results from Trout Beck suggest a temporal consistency in peat block size.

We suggest that the natural variation in peat block size and shape is influenced by three key factors: (i) the block delivery mechanism that imparts a control on the initial, unmodified peat block; (ii) the flow history that acts to modify peat blocks during in-channel processing; and (iii) the residence time of the peat block in the channel environment between transport events. Cantilever failure of peat banks is identified to be the principal delivery mechanism for peat blocks at Trout Beck (Evans and Warburton, 2001). This will provide initial peat blocks with highly variable physical characteristics, analogous to the complex assemblages of basal slump blocks in alluvial channels (Hackney *et al.*, 2015). The material properties of the source material will exert a control on peat block shape, with peat blocks sourced from the fibrous upper layer of the blanket peatland likely to have a more tabular

shape, whereas peat blocks sourced from the basal lower peat likely have a more equant shape. Following entrainment, in-channel processing will rework and modify the physical characteristics of peat blocks, with mechanical breakdown through splitting, breakage and abrasion (Figure 2). Experimental work has suggested that a critical submergence depth equivalent to peat block depth is required to initiate peat block movement (Warburton and Evans, 2001). The potential for entrainment, and consequently the extent of reworking and modification, will therefore depend on the hydraulic surface and flow velocity. Flow conditions in the lead up to the temporally independent inventories differed, with the peak daily flow in the 12 months preceding the 2012 inventory more than double that of the 2002 inventory (2002 = 4.88 m^3/s; 2012 = 11.7 m^3/s). Hence, the temporal sequencing of flow events would impart a control on the physical characteristics observed. Finally, significant hiatuses between peat block delivery, eventual entrainment/re-entrainment and deposition could result in further modifications of peat blocks. Recently delivered or deposited peat blocks that remain stationary but immersed in water for extended time periods have material removed during geomorphologically effective flow events (Wood *et al.*, 2001), so flow exposure may modify the physical characteristics. In addition, peat blocks will be exposed to progressive breakdown and weathering through wetting and drying, freeze-thaw, ice-needle growth and rainfall events which may significantly alter their physical characteristics and surface texture (Evans and Warburton 2001; Evans and Warburton, 2007; Li *et al.*, 2018). These three factors likely influence the physical characteristics of peat blocks observed in upland fluvial peatland ecosystems.

Following the link discontinuity concept (Rice and Church, 1998), mapped peat sources provide significant lateral input of peat blocks, with channel reaches between the inputs acting as sedimentary links. However, downstream fining over the study reach is disrupted by internal hydraulic peat block sorting sequences associated with preferential deposition on mid-channel bars and clustering on the floodplain (Figure 4, 8 and 9). Analogous to downstream fining in gravel-bed rivers, considerable noise can be introduced by complex sedimentary features that build up during numerous flow events of various magnitude, with different sizes of material supplied from upstream (Hoey and Bluck, 1999). This disruption explains the observed variation in downstream fining over the sedimentary

links (e.g. at 150-200 m downstream in Figure 8) and is inherent to the longitudinal distribution of peat blocks in upland fluvial peatland ecosystems.

Hypsometric relations show an underlying spatial organisation of peat blocks across the study reach with small changes in the hydraulic surface and/or local obstructions from topography, roughness and slope promoting rapid peat block deposition proximal to the active channel margin. The tight range of heights and uniform vertical distribution above the channel thalweg record the sensitivity to changes in hydraulic surface and support rapid deposition by stalling (Figure 2). Flow diversion and localised reductions of flow velocity have been associated with the deposition of peat blocks (Newall and Hughes, 1995; Evans and Warburton, 2001). In-channel and floodplain roughness elements may enhance the likelihood of deposition, as evidenced by the clustering of peat blocks on mid-channel bars (Figure 4). Interactions between floodplain vegetation (e.g. sedge patches) and flow could cause localised velocity reductions, heightening the potential for peat block deposition at the active channel margin (Evans and Warburton, 2001). Lateral heterogeneities in roughness elements surrounding the active channel contribute to the spatial organisation of peat blocks at Trout Beck, influencing peat block transport efficiency and their potential fate (i.e. potential for incorporation into the floodplain stratigraphic sequence).

Photo archive evidence from the lower section of the Trout Beck study reach showed that 74% of deposited peat blocks in the period 1997-2008 were re-entrained back into the flow, rather than buried into the floodplain stratigraphic sequence (Warburton and Evans, 2011). Hypsometric relations show that peat blocks are deposited proximal to the active channel margin, where the re-entrainment potential is high. Once entrained, the rates of peat block degradation are high (particularly through abrasion), so peat blocks can constitute a significant source of fine sediment release (Evans and Warburton, 2007). With the volume of peat blocks periodically renewed by bank and bluff erosion, peat blocks represent a dynamic component of the fluvially derived sediment and organic matter budget (Evans and Warburton, 2001; Crowe and Warburton, 2007).

Our inventories show that peat blocks represent a significant volume of fluvially derived in-channel

sediment at the macroscale (11 m^3 in 2002 and 17 m^3 in 2012). The first-order approximations of peat block degradation rates indicate considerable fine sediment release during transport; while photo archive imagery and hypsometric relations at this site suggest that floodplain burial is unlikely. In compiling a sediment budget for the nearby Rough Sike catchment (0.83 km^2, North Pennines; United Kingdom), Evans and Warburton (2005) showed a net sediment input of 8 m^3 was delivered annually as peat blocks from an actively failing peat bank (33 m in length). At the catchment scale, the volume of bank erosion at Rough Sike (and therefore fine sediment release) was budgeted to be 28.5 m^3 a^{-1}. For the larger Trout Beck catchment (11.4 km^2), we estimate that comparable volumes of fine sediment are released from the transport and in-channel processing of peat blocks along a single actively eroding alluvial reach (e.g. DR3 in 2012, Table 3). Peat blocks are not only morphologically important but also represent an important source of fine sediment in peatland ecosystems. Although this sediment flux is widely recognised, the contribution of peat blocks to catchment sediment budgets represent a significant knowledge gap (Evans and Burt 2010).

With high peat block transport efficiencies, peat blocks can rapidly degrade and release organic material (Crowe and Warburton, 2007). Given the low potential for storage in channel beds, this organic material is exported from the catchment so represents a significant loss of terrestrial carbon (Crowe and Warburton, 2007). Carbon sequestration can take place if peat blocks are eventually incorporated into the sedimentary sequence (Evans and Lindsay 2010; Warburton and Evans, 2011), but results from the Trout Beck study reach suggest this is unlikely. Crucially, carbon budget studies are increasingly used by upland managers to inform and implement land strategies on carbon stewardship, with the fluvial component the second largest contributor to the upland terrestrial carbon budget (Warburton and Evans 2011). Omission of the fluvial component could lead to a significant underestimation of the total carbon flux (Webster and Meyer, 1997), and here we advocate for recognition of the BOC component within such budgets. Further field and flume experimentation are needed for the quantification of peat block entrainment thresholds, transport phases and detailed degradation losses (both fine sediment and organic carbon). The implications for large peat blocks in catchment sediment budgets and organic carbon cascades are particularly relevant given that blanket

peatlands have experienced severe erosion and will experience an increasing erosion risk from 21st century climate change (Evans and Warburton, 2007; Li *et al.*, 2016; Li *et al.*, 2017); raised awareness and improved process-understanding for this phenomena is therefore vital.

5. Conclusions

This paper has investigated the physical characteristics (size and shape) and spatial organisation of peat blocks in an upland peatland dissected by fluvial erosion. Through collection of two temporally independent peat block inventories, first-order approximations of peat block degradation rates and estimates of fine sediment release have been provided. Key findings include:

1. Peat blocks are variable in size, with orthogonal axis dimensions on the order of centimetres to meters. Peat block a-axes typically exceed the b-axes by 1.5-2 and a range of peat block shapes are classified. The proportion of classified peat block shapes varies between the temporally independent inventories (e.g. equant shaped blocks represent 5% of the total in 2002, 42% in 2012), but the size (b-axis and volume) remains temporally coherent.
2. Peat blocks represent a substantial volume of fluvially derived sediment and carbon flux at the macroscale. The total volume of measured peat blocks was 10.50 m^3 in 2002, this increased by 59% to 16.68 m^3 in 2012.
3. Inferred peat block transport distances support a positive feedback with smaller and more spherical peat blocks are transported greater distances (Evans and Warburton, 2007). Equant shaped blocks are transported the greatest distances (125.60 m), have the smallest characteristic size and have the most spherical morphology. Shorter average transport distances are shown for prolate (77.59 m) and elongate (73.23 m) shaped blocks. Prolate shaped blocks have a larger average block volume and more rod-like morphology; whereas elongate shaped blocks have the lowest sphericity. In addition to a size-control, the shape and morphology of peat blocks influence transmission through fluvial systems.
4. Downstream fining relationships provide a first-order approximation for peat block degradation rates, these are high (up to 2 mm/m for the a-axis) and indicate considerable fine

sediment release during peat block transport (e.g. DR3: 9.64 m^3 in 2002; 32.08 m^3 in 2012).

5. Hypsometric relations show a spatial organisation of peat blocks across the study reach. 73% of peat blocks are distributed within 1 channel width of the channel thalweg, indicative of preferential deposition proximal to the active channel margin.
6. Future work is needed to improve the process-understanding of peat block of transmission and in-channel processing. This includes field and flume experimentation for the quantification of peat block entrainment thresholds, transport phases and detailed degradation losses (sediment and organic carbon). This is necessary to better constrain catchment sediment budgets and organic carbon cascades in actively eroding, fluvially-dissected upland peatland ecosystems.

Acknowledgments

We would like to thank Natural England and UK Centre for Ecology & Hydrology ECN Central Coordination Unit for access to the Moor House National Nature Reserve and co-operation. Work related to this project was partly funded by a NERC (NE/F010141/1) award to JW. We are grateful to Mark Kincey and Sarah Crowe for access to unpublished data. We would like to thank Rich Hardy for helpful comments on an earlier version of this manuscript. The authors are grateful to the Editor and two anonymous reviewers for providing helpful comments that led to significant improvements in this manuscript.

Data availability

Data used in this manuscript can be obtained by contacting the lead author.

References

Aitkenhead, N., Barclay, W.J., Brandon, A., Chadwick, R.A., Chisholm, J.I., Cooper, A.H., Johnson, E.W., 2002. British Regional Geology: The Pennines and Adjacent Areas. British Geological Society, Nottingham.

Alderson, D.M., Evans, M.G., Rothwell, J.J., Rhodes, E.J., Boult, S., 2019. Geomorphological controls on fluvial carbon storage in headwater peatlands. Earth Surface Processes and Landforms. 44(9), pp. 1675-1693.

Aspray, K.L., Holden, J., Ledger, M.E., Mainstone, C.P., Brown, L.E., 2017. Organic sediment pulses impact rivers across multiple levels of ecological organization. Ecohydrology. 10(6), e1855.

Beisel, J-N., Usseglio-Polatera, P., Moreteau, J-C., 2000. The spatial heterogeneity of a river bottom: a key factor determining macroinvertebrate communities. Hydrobiologia. 422-423, pp. 163-171.

Bouckaert, F.W., Davis, J., 1998. Microflow regimes and the distribution of macroinvertebrates around stream boulders. Freshwater Biology. 40(1), pp. 77-86.

Bower, M.M., 1961. The Distribution of Erosion in Blanket Peat Bogs in the Pennines. Transactions and Papers (Institute of British Geographers). 29, pp. 17-30.

Brown, L.E., Aspray, K.L., Ledger, M.E., Mainstone, C.P., Palmer, S.M., Wilkes, M., Holden, J., 2019. Sediment deposition from eroding peatlands alters headwater invertebrate biodiversity. Global Change Biology. 25(2), pp. 602-619.

Conway, V.M., 1954. Stratigraphy and Pollen Analysis of Southern Pennine Blanket Peats. Journal of Ecology. 42(1), pp. 117-147.

Crowe, S., Warburton, J., 2007. Significance of large peat blocks for river channel habitat and stream organic budgets. Mires and Peat. 2, pp. 1-15.

Davis, J.A., Barmuta, L.A., 1989. An ecologically useful classification of mean and near-bed flows in streams and rivers. Freshwater Biology. 21(2), pp. 271-282.

Dykes, A.P., Warburton, J., 2007. Mass movements in peat: A formal classification scheme. Geomorphology. 86(1-2), pp. 73-93.

Dykes, A.P., Warburton, J., 2008. Characteristics of the Shetland Islands (UK) peat slides of 19 September 2003. Landslides. 5(2), pp. 213-226.

Evans, M., Burt, T.P., 2010. Erosional Processes and Sediment Transport in Upland Mires, in: Burt, T., Allison, R., (eds), Sediment Cascades: An Integrated Approach. Wiley, Hoboken, pp. 217-240.

Evans, M., Lindsay, J., 2010. High resolution quantification of gully erosion in upland peatlands at the landscape scale. Earth Surface Processes and Landforms. 35(8), pp. 876-886.

Evans, M., Warburton, J., 2001. Transport and dispersal of organic debris (peat blocks) in upland fluvial systems. Earth Surface Processes and Landforms. 26(10), pp. 1087-1102.

Evans, M., Warburton, J., 2005. Sediment budget for an eroding peat-moorland catchment in northern England. Earth Surface Processes and Landforms. 30(5), pp. 557-577.

Evans, M., Warburton, J., 2007. The geomorphology of upland peat: erosion, form and landscape. Blackwell, Oxford.

Evans, M., Warburton, J., Yang, J., 2006. Eroding blanket peat catchments: Global and local implications of upland organic sediment budgets. Geomorphology. 79(1-2), pp. 45-57.

Evans, M., Warburton, J., 2010. Peatland Geomorphology and Carbon Cycling. Geography Compass. 4(10), pp. 1513-1531.

Ferguson, R.I., Sharma, B.P., Hardy, R.J., Hodge, R.A., Warburton, J., 2017. Flow resistance and hydraulic geometry in contrasting reaches of a bedrock channel. Water Resources Research. 53(3), pp.

2278-2293.

Ferguson, R.I., Hardy, R.J. Hodge, R.A.. 2019. Flow resistance and hydraulic geometry in bedrock rivers with multiple roughness length scales. Earth Surface Processes and Landforms, 44(12), pp.2437-2449.

Garnett, M.H., Adamson, J.K., 1997. Blanket mire monitoring and research at Moor House Nature Reserve. Macaulay Land Use Research Institute, Aberdeen.

Garnett, M., Adamson, J.K., 1997. Blanket mire monitoring and research at Moor House National Nature Reserve, in: Tallis, J.H., Meade, R., Hulme, P.D., (eds), Blanket Mire Degradation: Causes and Consequences. British Ecological Society, Aberdeen, pp. 116-117.

Hackney, C., Best, J., Leyland, J., Darby, S.E., Parsons, D., Aalto, R., 2015. Modulation of outer bank erosion by slump blocks: Disentangling the protective and destructive role of failed material on the three-dimensional flow structure. Geophysical Research Letters. 42, pp. 10663-10670.

Hoey, T.B., Bluck, B.J., 1999. Identifying the controls over downstream fining of river gravels. Journal of Sedimentary Research. 69(1), pp. 40-50.

Holden, J., Burt, T.P., 2003. Runoff production in blanket peat covered catchments. Water Resources Research. 39(7), 1191.

Johnson, G.A.L., Dunham, K.C., 1963. The geology of Moor House. Monographs of the Nature Conservancy Council Number Two. HMSO, London.

Illenberger, W.K., 1991. Pebble shape (and size?). Journal of Sedimentary Research. 61(5), pp. 756-767.

IPCC., 2018: Global warming of 1.5°C. An IPCC Special Report on the impacts of global warming of 1.5°C above pre-industrial levels and related global greenhouse gas emission pathways, in the context of strengthening the global response to the threat of climate change, sustainable development, and efforts to eradicate poverty. Available at: http://ipcc.ch/report/sr15/ (accessed 20 March 2020).

Labadz, J.C., Burt, T.P., Potter, A.W.R., 1991. Sediment yield and delivery in the blanket peat moorlands of the southern Pennines. Earth Surface Processes and Landforms. 16(3), pp. 255-271.

Li, P., Holden, J., Irvine, B., 2016. Prediction of blanket peat erosion across Great Britain under environmental change. Climate Change. 134(1-2), pp. 177-191.

Li, P., Holden, J., Irvine, B., Mu, X., 2017. Erosion of Northern Hemisphere blanket peatlands under 21st-century climate change. Geophysical Research Letters. 44(8), pp. 3615-3623.

Li, C., Holden, J., Grayson, R., 2018. Effects of needle ice on peat erosion processes during overland flow events. Journal of Geophysical Research: Earth Surface. 123(9), pp. 2107-2122.

Lindsay, R., 2010. Peatbogs and carbon: acritical synthesis to inform policy development in oceanic peat bog conservation and restoration in the context of climate change. Environmental Research Group, University of East London.

Moody, C.S., Worrall, F., Evans, C.D., Jones, T., 2013. The rate of loss of dissolved organic carbon (DOC) through a catchment. Journal of Hydrology. 492, pp. 139-150.

Newall, A.M., Hughes, J.M.R., 1995. Microflow environments of aquatic plants in flowing water wetlands, in: Hughes, J.M.R., Heathwaite, A.L., (eds). Hydrology and Hydrochemistry of British Wetlands. Wiley, Chichester, pp. 363-381.

National River Flow Archive (NRFA). 2020. 25003 - Trout Beck at Moor House. Accessed July 2020: https://nrfa.ceh.ac.uk/data/station/meanflow/25003

Passy, S.I., 2001. Spatial paradigms of lotic diatom distribution: a landscape ecology perspective. Journal of Phycology. 37(3), pp. 370-378.

Pawson, R.R., 2008. Assessing the role of particulates in the fluvial organic carbon flux from eroding peatland systems. PhD thesis, University of Manchester.

Pawson, R.R., Lord, D.R., Evans, M., Allott, T.E.H., 2008. Fluvial organic carbon flux from an eroding peatland catchment, southern Pennines, UK. Hydrology and Earth System Science. 12(2), pp. 625-634.

Pawson, R.R., Evans, M., Allott, T.E.H., 2012. Fluvial carbon flux from headwater peatland streams: significance of particulate carbon flux. Earth Surface Processes and Landforms. 37(11), pp. 1203-1212.

Planet Team., 2017. Planet Application Program Interface: In Space for Life on Earth. San Francisco, CA. https://api.planet.com.

Ramchunder, S. J., Brown, L. E., Holden, J., 2012. Catchment-scale peatland restoration benefits stream ecosystem biodiversity. Journal of Applied Ecology. 49, pp. 182-191.

Rice, S.P., Church, M., 1998. Grain size along two gravel-bed rivers: statistical variation, spatial pattern and sedimentary links. Earth Surface Processes and Landforms. 23(4), pp. 345-363.

Rice, S.P., Greenwood, M.T., Joyce, C.B., 2001. Tributaries, sediment sources, and the longitudinal organisation of macroinvertebrate fauna along river systems. Canadian Journal of Fisheries and Aquatic Sciences. 58(4), pp. 824-840.

Sneed, E.D., Folk, R.L., 1958. Pebbles in the lower Colorado River, Texas a study in Particle Morfogenesis. Journal of Geology. 66(2), pp. 114-150.

Townsend, C.R., 1989. The Patch Dynamics Concept of Stream Community Ecology. Journal of the North American Benthological Society. 8(1), pp. 36-50.

Walling, D.E., 1983. The sediment delivery problem. Journal of Hydrology. 65(1-3), pp. 209-237.

Walker, J., Lennart, A., Peippo, J., 1987. Riverbank Erosion in the Colville Delta, Alaska. Geografiska Annaler. 69(1), pp. 711–720.

Warburton, J., Evans, M., 2011. Geomorphic, sedimentary, and potential palaeoenvironmental significance of peat blocks in alluvial river systems. Geomorphology. 130(3-4), pp. 101-114.

Webster, J.R., Meyer, J.L., 1997. Stream Organic Matter Budgets: An Introduction. Journal of the North American Benthological Society. 16(1), pp. 3-13.

Worrall, F., Burt, T.P., Rowson, J.G., Warburton, J., Adamson, J.K., 2009. The multi-annual carbon budget of a peat-covered catchment. Science of The Total Environment. 407(13), pp. 4084-4094.

Table 1 – Summary statistics of peat block size and inferred transport distances for the 2002, 2012 and combined inventories.

Inventory	Dimension	Mean	Median	Range	Standard deviation	Skewness	Kurtosis	Number of blocks
2002	*a-axis (m)*	0.69	0.52	2.93	0.54	2.39	9.43	123
	b-axis (m)	0.32	0.28	0.97	0.17	0.96	4.35	
	c-axis (m)	0.18	0.15	0.51	0.11	0.79	3.05	
	Volume (m^3)	0.09	0.02	1.07	0.17	3.75	19.01	
	Inferred transport distance (m)	64.07	60.00	340.00	47.77	1.73	8.17	
2012	*a-axis (m)*	0.64	0.59	2.12	0.37	1.49	6.15	127
	b-axis (m)	0.42	0.41	1.08	0.20	1.08	4.34	
	c-axis (m)	0.28	0.25	0.73	0.13	1.26	5.22	
	Volume (m^3)	0.13	0.06	1.59	0.24	4.21	23.11	
	Inferred transport distance (m)	120.79	111.84	193.97	55.46	-0.27	-1.07	
Combined	*a-axis (m)*	0.66	0.55	2.93	0.46	2.31	10.21	250
	b-axis (m)	0.37	0.34	1.13	0.19	1.06	4.54	
	c-axis (m)	0.23	0.21	0.80	0.13	1.03	4.72	
	Volume (m^3)	0.11	0.06	1.59	0.21	4.32	25.48	
	Inferred transport distance (m)	92.86	93.21	340.73	59.01	0.49	0.08	

Table 2 – Peat block size (b-axis and volume), morphology (Corey shape index and disk-rod index) and inferred distance from peat source for the classified peat block shapes in the 2002, 2012 and combined inventories.

Inventory	Peat block shape	Count	b-axis (m)		Volume (m^3)		Corey shape index (-)		Disk-rod index (-)		Inferred transport distance (m)	
			Mean	Standard deviation	Mean	Standard deviation	Mean	Standard deviation	Mean	Standard deviation	Mean	Standard deviation
2002	*Elongate*	57	0.31	0.17	0.07	0.12	0.34	0.09	0.70	0.11	62.63	40.18
	Equant	6	0.36	0.13	0.06	0.05	0.65	0.03	0.55	0.13	44.17	25.18
	Prolate	33	0.30	0.18	0.14	0.26	0.49	0.10	0.86	0.09	48.03	40.46
	Tabular	27	0.36	0.18	0.05	0.09	0.38	0.13	0.38	0.16	91.11	62.55
2012	*Elongate*	21	0.45	0.15	0.15	0.20	0.40	0.07	0.62	0.07	102.00	62.18
	Equant	53	0.34	0.19	0.09	0.22	0.74	0.09	0.60	0.22	134.82	54.99
	Prolate	25	0.45	0.21	0.24	0.36	0.60	0.08	0.83	0.08	116.61	48.52
	Tabular	28	0.53	0.19	0.12	0.10	0.45	0.10	0.35	0.15	112.06	53.08
Combined	*Elongate*	78	0.35	0.18	0.09	0.15	0.36	0.08	0.68	0.11	73.23	49.87
	Equant	59	0.34	0.19	0.08	0.21	0.73	0.09	0.60	0.21	125.60	59.41
	Prolate	58	0.37	0.21	0.18	0.31	0.54	0.11	0.84	0.08	77.59	55.54
	Tabular	55	0.45	0.20	0.08	0.10	0.42	0.12	0.32	0.15	101.78	58.34

Table 3 – Estimated fine sediment release under peat block degradation rate scenarios for the 2002, 2012 and combined inventories.

Inventory	Degradation rate scenario	a-axis degradation rate (mm/m)	b-axis degradation rate (mm/m)	c-axis degradation rate (mm/m)	Estimated pre-transport volume of peat blocks, (m^3)	Estimated volume of fine sediment released (m^3)	% of pre-transport volume released as fine sediment
2002	Surveyed	-	-	-	10.50	-	-
	DR1	0.5	0.5	0.5	12.16	1.66	13.67
	DR2	1	1	1	14.27	3.77	26.41
	DR3	2	2	2	20.14	9.64	47.86
	DR4	4	4	4	40.79	30.29	74.26
	DR5	2	0	0	11.46	0.96	8.37
	DR6	2	1	0.5	13.89	3.39	24.41
	DR7	4	2	1	19.24	8.74	45.42
2012	Surveyed	-	-	-	16.68	-	-
	DR1	0.5	0.5	0.5	22.02	5.34	24.25
	DR2	1	1	1	28.96	12.29	42.42
	DR3	2	2	2	48.76	32.08	65.8
	DR4	4	4	4	119.49	102.81	86.04
	DR5	2	0	0	20.54	3.86	18.79
	DR6	2	1	0.5	28.66	11.99	41.81
	DR7	4	2	1	48.09	31.41	65.32
Combined	Surveyed	-	-	-	27.18	-	-
	DR1	0.5	0.5	0.5	34.18	7.00	20.48
	DR2	1	1	1	43.23	16.05	37.14
	DR3	2	2	2	68.9	41.72	60.56
	DR4	4	4	4	160.28	133.1	83.04
	DR5	2	0	0	32.00	4.82	15.06
	DR6	2	1	0.5	42.55	15.38	36.13
	DR7	4	2	1	67.33	40.15	59.64

Figures

Figure 1 – Examples of peat blocks from a range of environmental settings, including: (a) source bank failures (Trout Beck, North Pennines, UK); (b) source peat landslide (Dooncarton, Western Ireland); (c) spatial organisation across an active channel margin (Trout Beck, North Pennines, UK); (d) weathering and erosion in-situ (Upper Tees, North Pennines, UK); (e) abraded elongate 'spindle-form' peat block (Trout Beck, North Pennines, UK); and (f) elongate peat block form (Severn Estuary, UK).

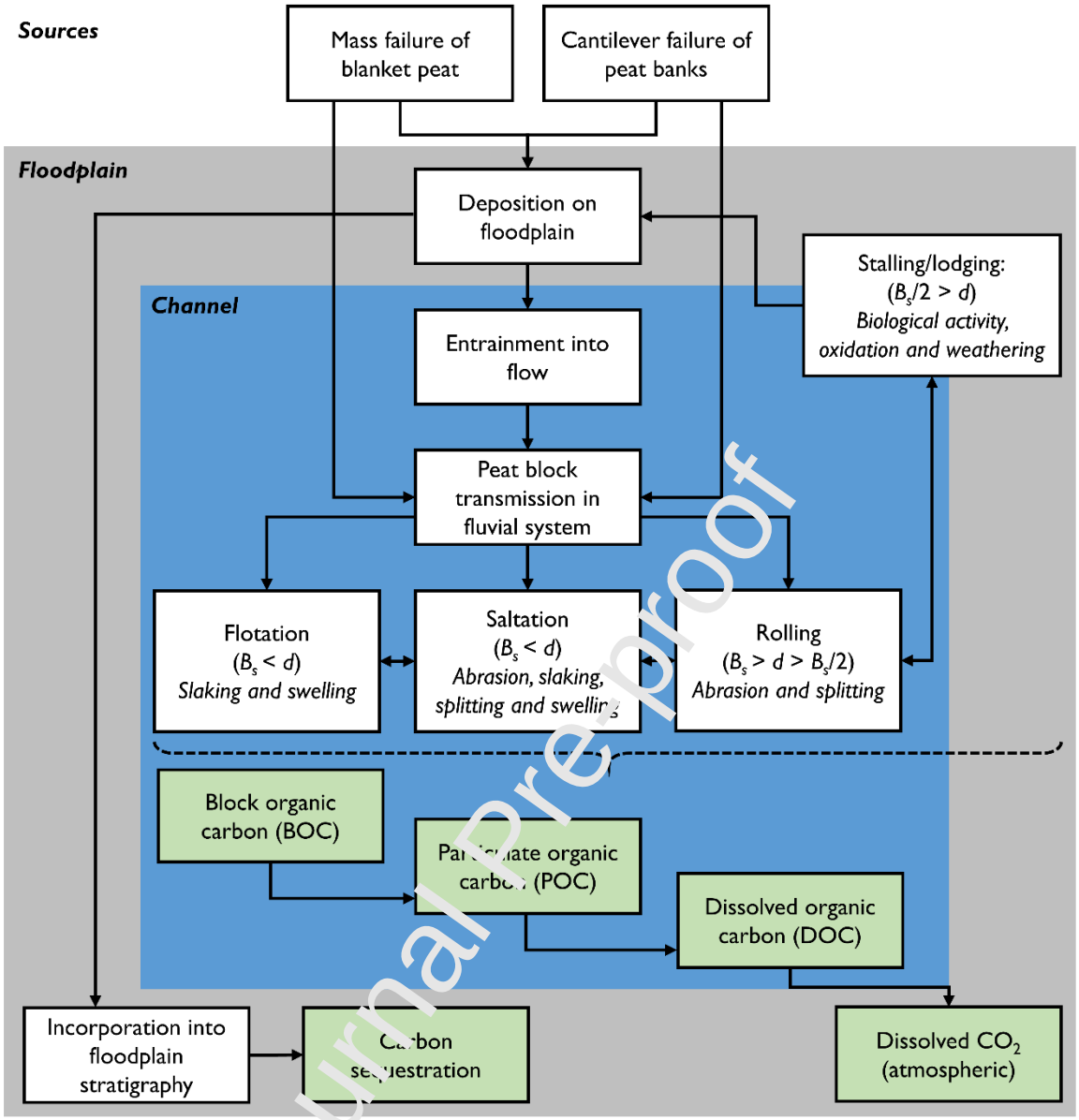

Figure 2 – Conceptual diagram showing the delivery, in-channel processing and organic carbon cascade of peat blocks through the fluvial system. Note distinction between channel (blue) and floodplain (grey) processes and organic carbon cascade (green). B_s refers to peat block size and d refers to flow depth (modified from Evans and Warburton, 2001).

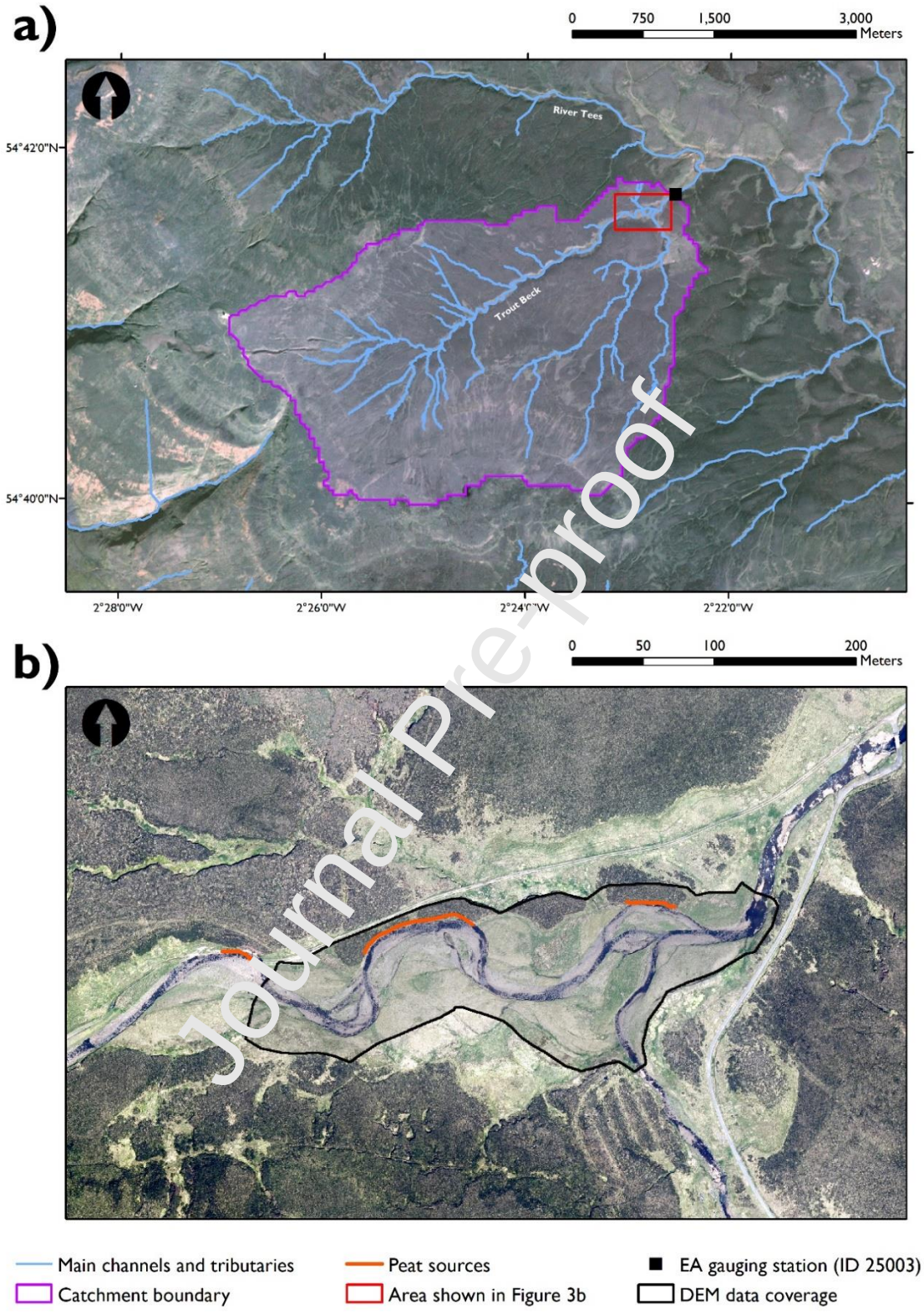

Figure 3 – Study site overview showing: (a) the Trout Beck catchment and the Environment Agency (EA) gauging station; and (b) the study reach. Data for the catchment boundary is from National River Flow Archive (NRFA, 2020), 3 m resolution PlanetScope satellite imagery acquired 10 October 2018 (Planet Team, 2017) and 2018 aerial imagery from Edina Digimap © Getmapping Plc.

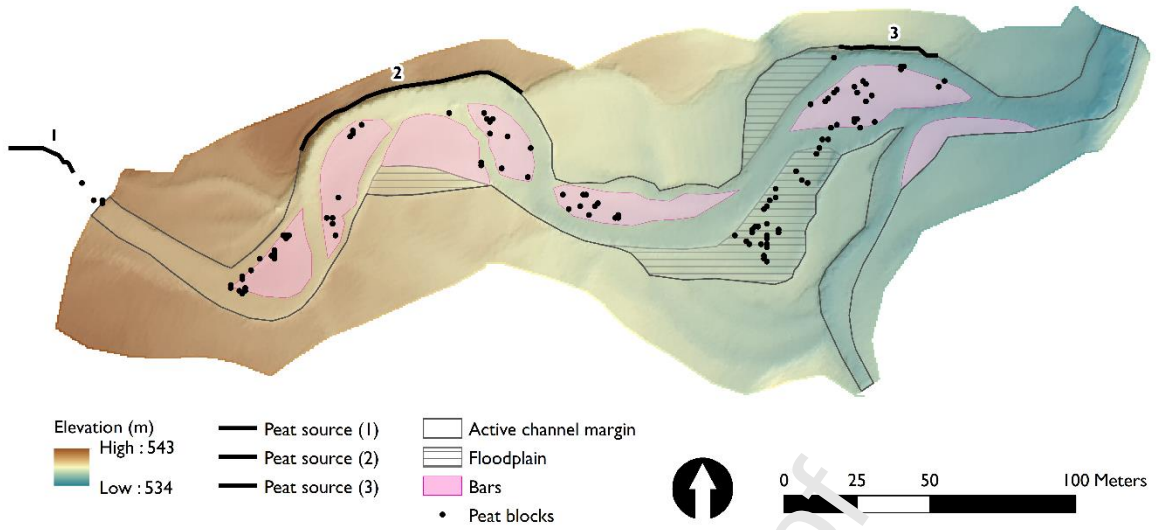

Figure 4 – Spatial distribution of peat blocks in the 2012 inventory (n = 127) overlaid on the hillshaded digital elevation model (DEM). Trout Beck flows from west to east. Identified peat sources are mapped and labelled (thick black lines) with several clusters of deposited peat blocks shown.

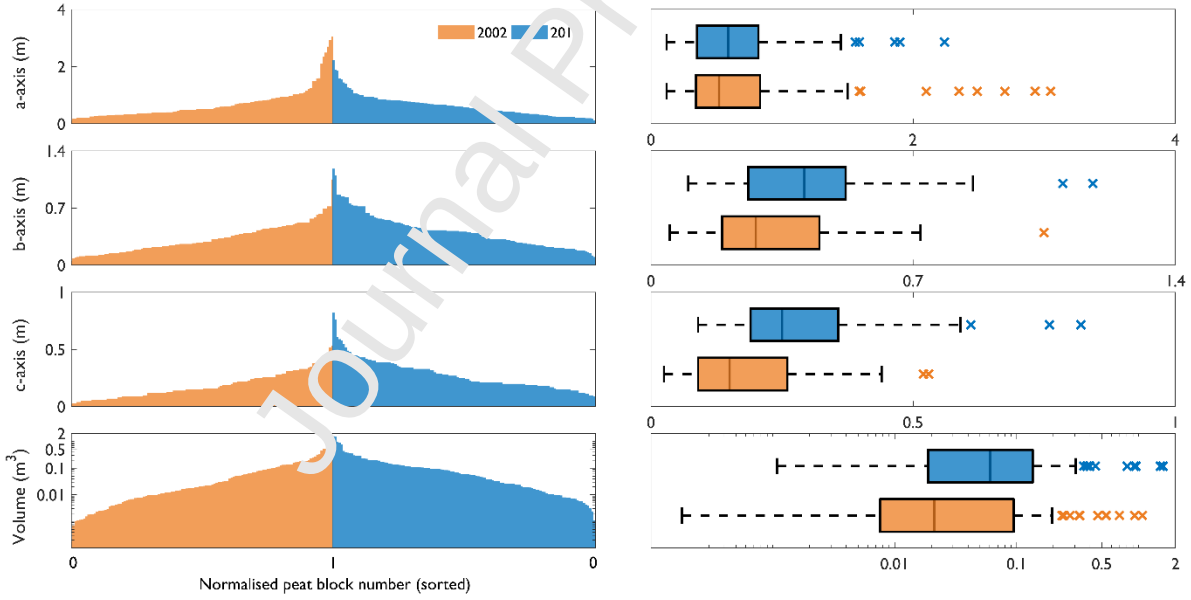

Figure 5 – Comparison of peat block size (orthogonal axes and volume) between the 2002 and 2012 inventories with peat blocks sorted smallest to largest and normalised by number sampled (n = 123 in 2002; n = 127 in 2012) and same data redrawn as boxplots. Note, same axis scale between plots. Approximately similar distributions are shown between the 2002 and 2012 inventories.

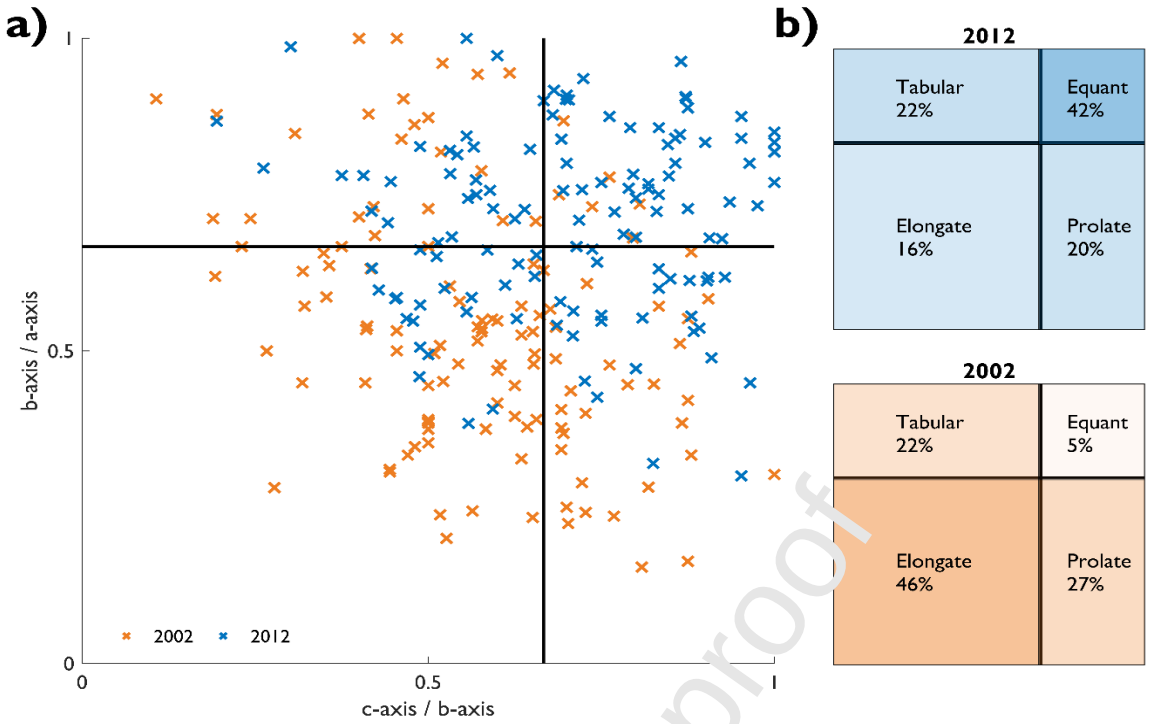

Figure 6 – Differences in peat block shape between the 2002 and 2012 inventories shown as: (a) Zingg-type diagrams; and (b) as a proportion of peat blocks classified for each block shape (colour intensity scales with the proportion of each peat block shape classified).

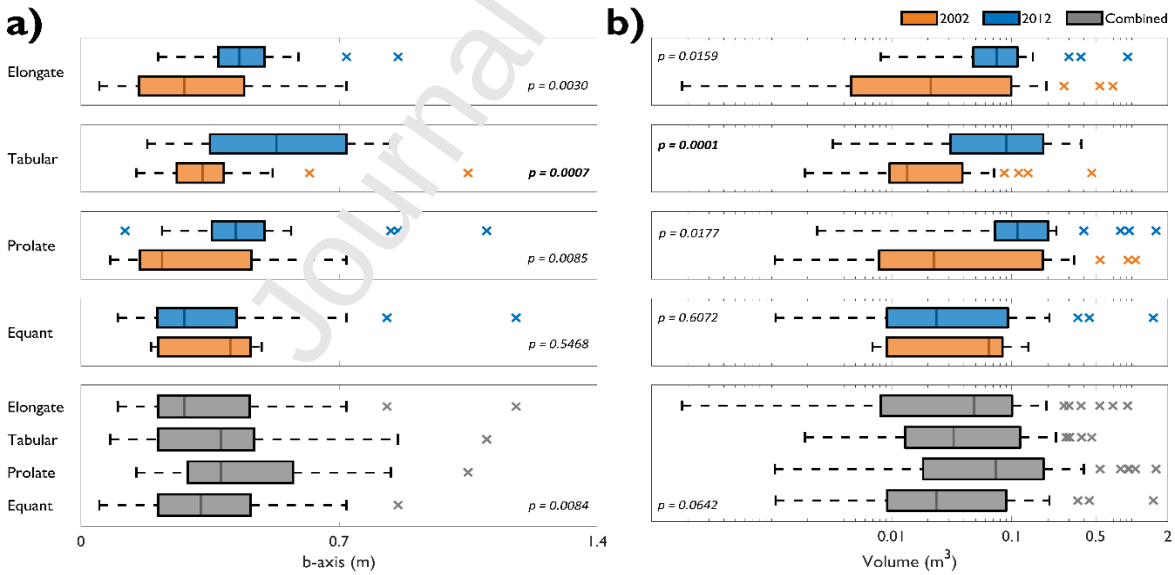

Figure 7 – Relationship between peat block size and classified shape. Peat block size is defined as: (a) b-axis; and (b) block volume. *P*-values show the results of Mann-Whitney tests for size between temporally independent peat block inventories, and Kruskal–Wallis tests between peat blocks of different classified shapes (significance is marked in bold, *p*-value < 0.001).

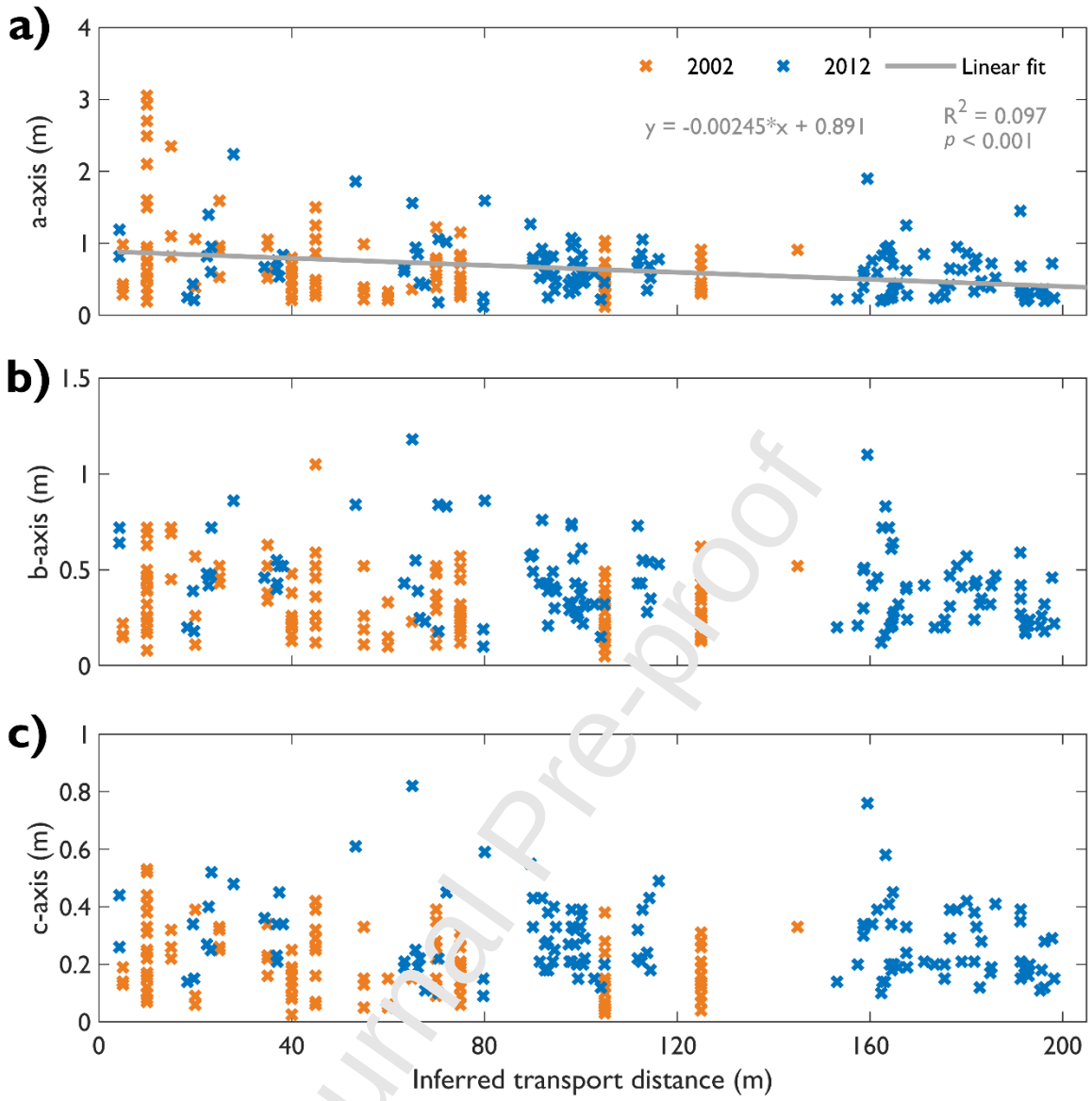

Figure 8 – Changes in peat block size (a) a-axis, (b) b-axis, (c) c-axis with inferred transport distance for the 2002 and 2012 inventories. The solid grey line represents the linear regression of the 2002 and 2012 combined inventories. Note that a single data point from the 2002 inventory at 345 m is not shown due to visual constraints but is included in the regression.

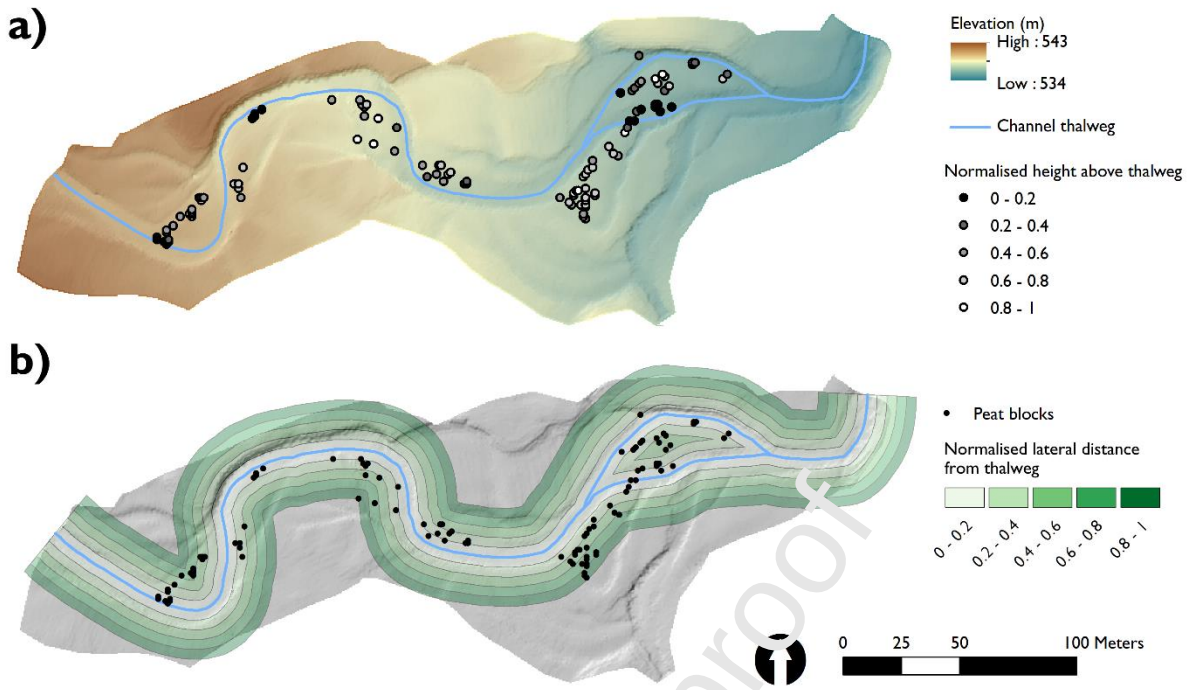

Figure 9 – Spatial distribution of peat blocks for the 2012 inventory, shown as: (a) normalised height above the channel thalweg; and (b) normalised lateral distance from the channel thalweg. Only peat blocks that were recorded within the DEM coverage area were included for analysis (n = 123).

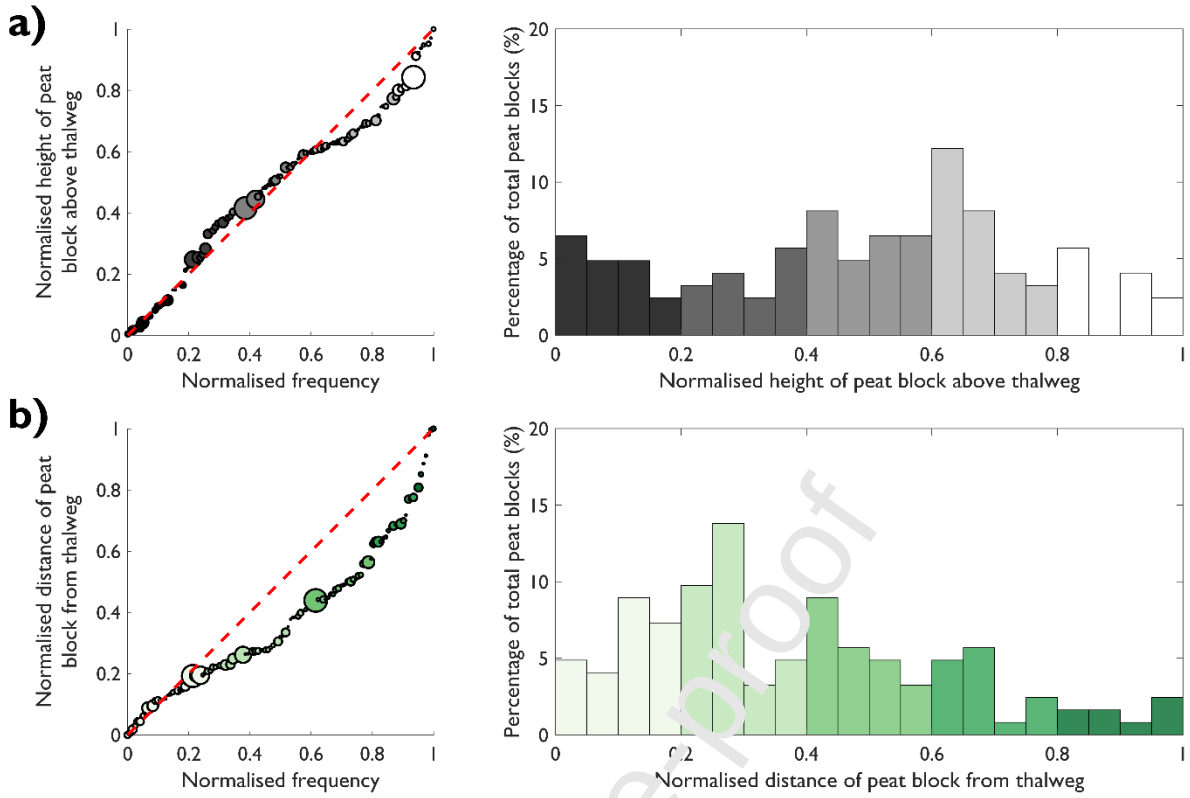

Figure 10 – Hypsometric relations of peat blocks from the 2012 inventory, shown as: (a) normalised height above the channel thalweg; and (b) normalised distance from the channel thalweg. Colour shading is the same is in Figure 9. Marker points are analytically weighted and proportional in radius to the peat block volume, the line of equality is shown as the red dashed line. Histograms show the percentage of peat blocks at each 0.05 normalised interval.

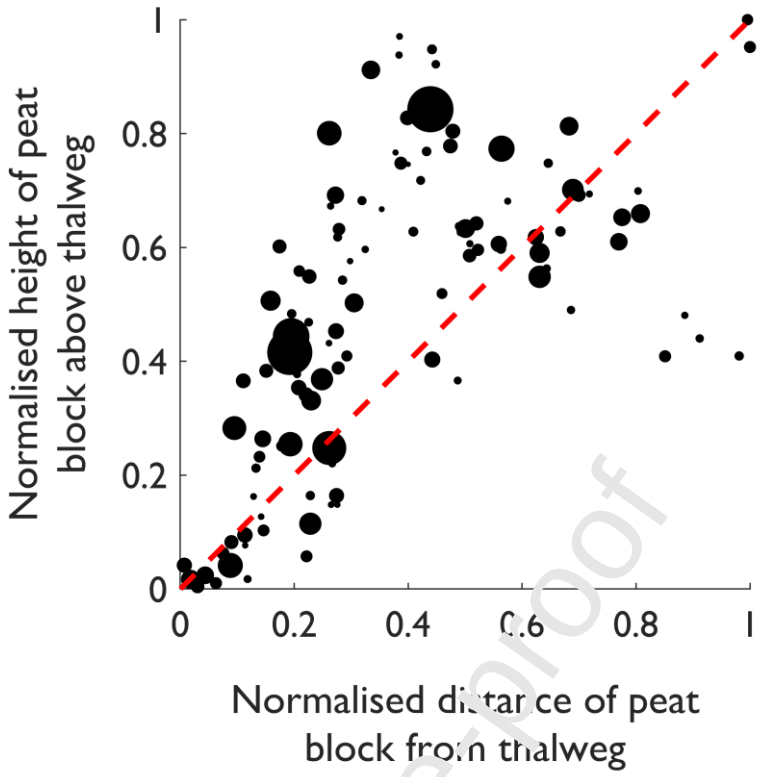

Figure 11 – Lateral and vertical organisation of mapped peat blocks from the 2012 inventory. Marker points are analytically weighted and proportional in radius to the peat block volume, the line of equality is shown as the red dashed line.

Declaration of competing interests

☒ The authors declare that they have no known competing financial interests or personal relationships that could have appeared to influence the work reported in this paper.

☐The authors declare the following financial interests/personal relationships which may be considered as potential competing interests:

Highlights

- Peat block (organic debris) inventories collected in an upland peatland ecosystem
- Represent a substantial volume of sediment and carbon flux at the macroscale
- High degradation rates indicate considerable fine sediment release during transport
- Preferentially deposited at the active channel margin where re-entrainment likely

Figure 1

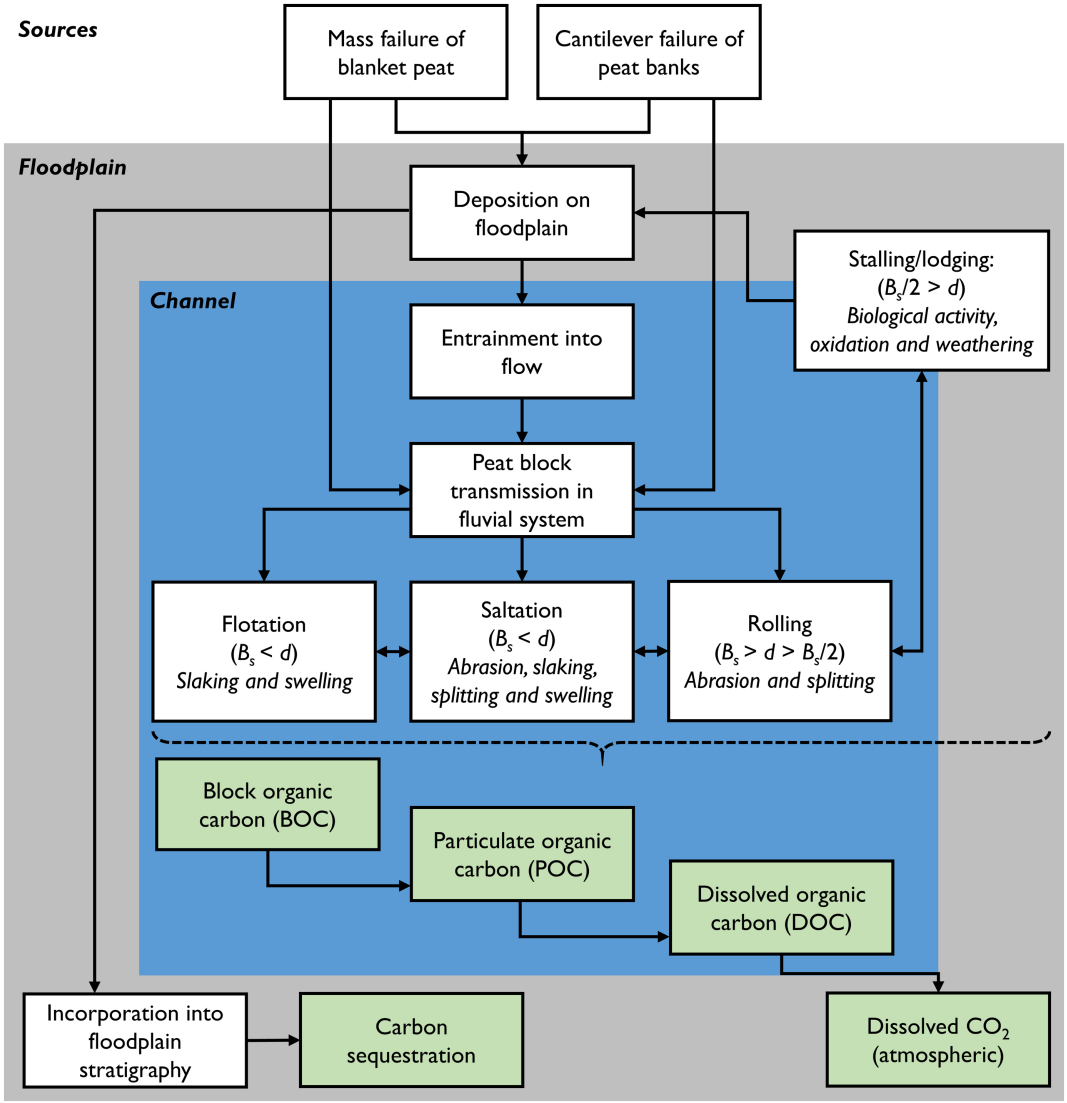
Sources
Mass failure of blanket peat
Cantilever failure of peat banks
Floodplain
Deposition on floodplain
Stalling/lodging: ($B_s/2 > d$) Biological activity, oxidation and weathering
Channel
Entrainment into flow
Peat block transmission in fluvial system
Flotation ($B_s < d$) Slaking and swelling
Saltation ($B_s < d$) Abrasion, slaking, splitting and swelling
Rolling ($B_s > d > B_s/2$) Abrasion and splitting
Block organic carbon (BOC)
Particulate organic carbon (POC)
Dissolved organic carbon (DOC)
Incorporation into floodplain stratigraphy
Carbon sequestration
Dissolved CO_2 (atmospheric)

Figure 2

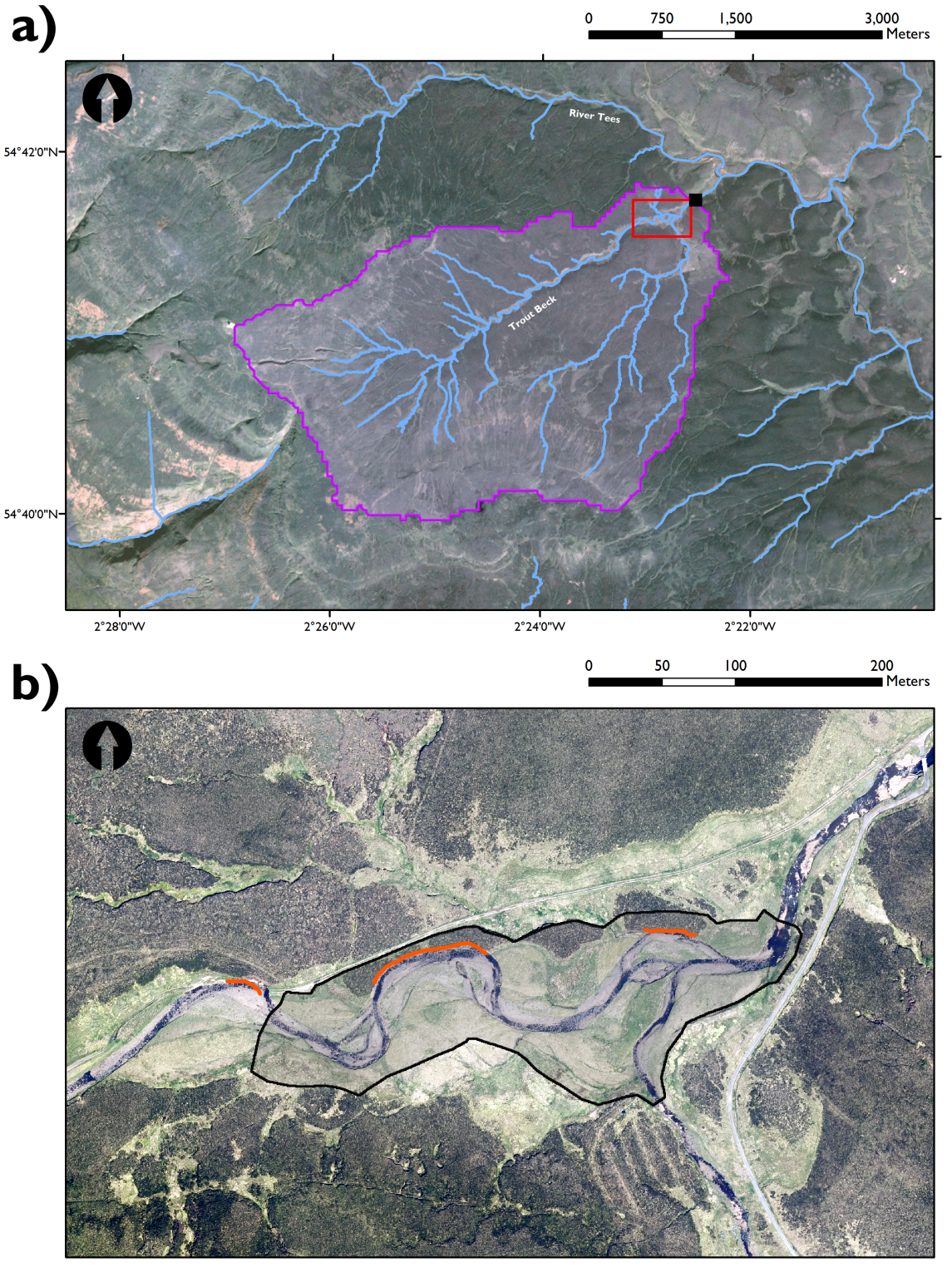
a)
0
750
1,500
3,000
Meters
River Tees
Trout Beck
54°42'0"N
54°40'0"N
2°28'0"W
2°26'0"W
2°24'0"W
2°22'0"W
b)
0
50
100
200
Meters
Main channels and tributaries
Peat sources
EA gauging station (ID 25003)
Catchment boundary
Area shown in Figure 3b
DEM data coverage

Figure 3

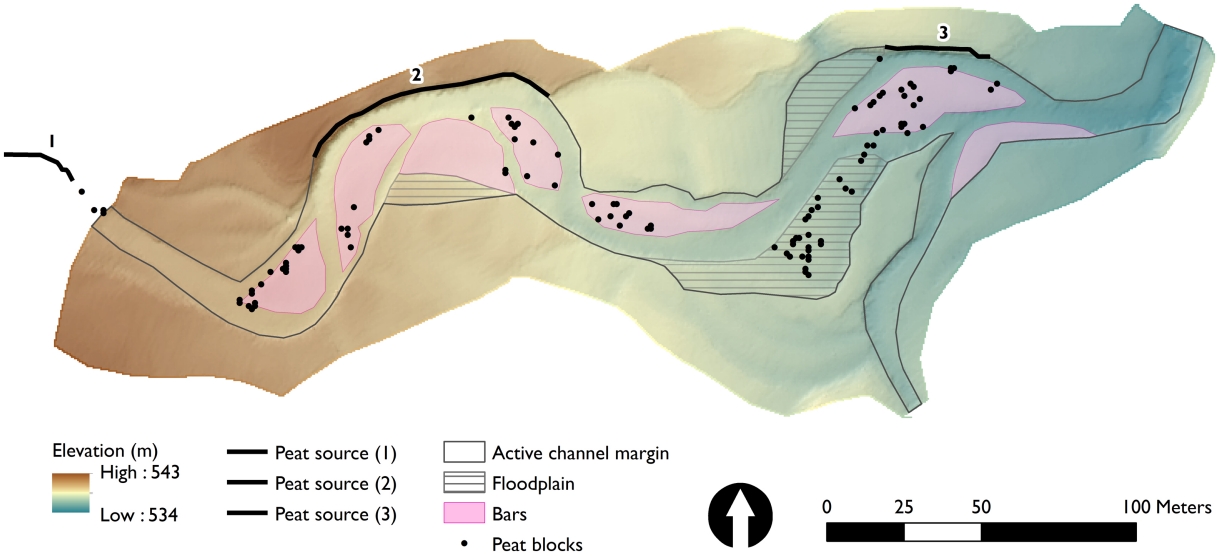
1
2
3
Elevation (m)
High : 543
Low : 534
Peat source (1)
Peat source (2)
Peat source (3)
Active channel margin
Floodplain
Bars
Peat blocks
0
25
50
100 Meters

Figure 4

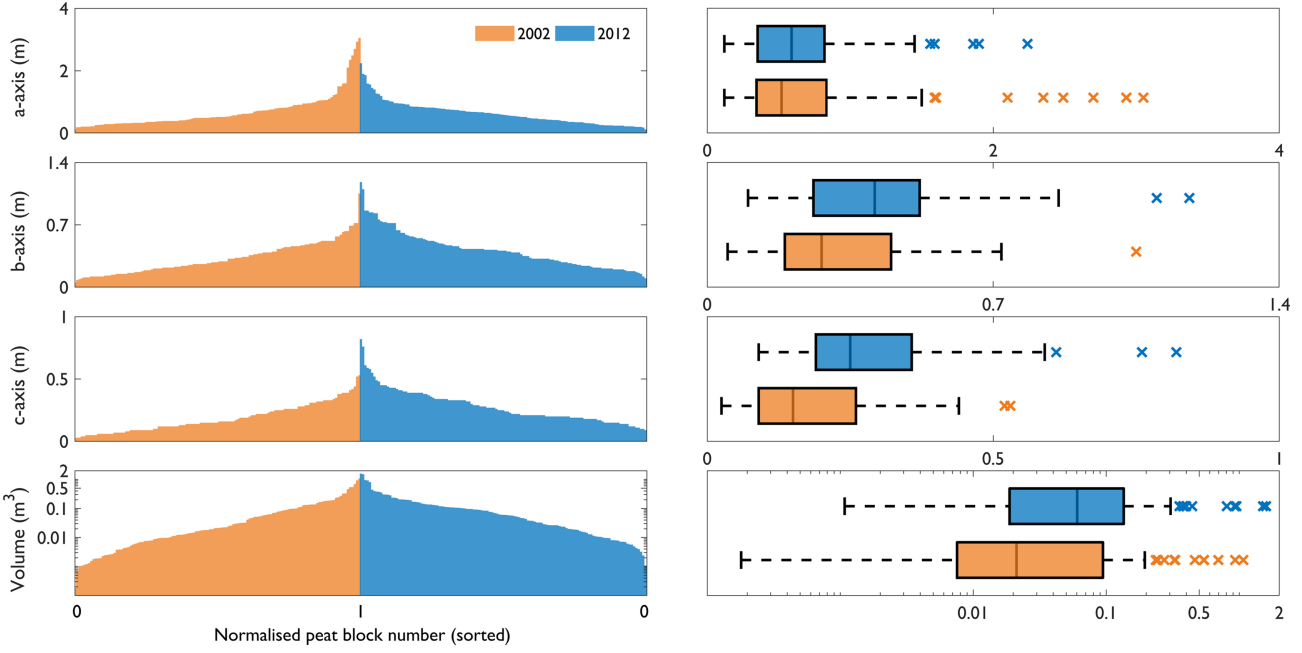
2002
2012
a-axis (m)
b-axis (m)
c-axis (m)
Volume (m3)
Normalised peat block number (sorted)

Figure 5

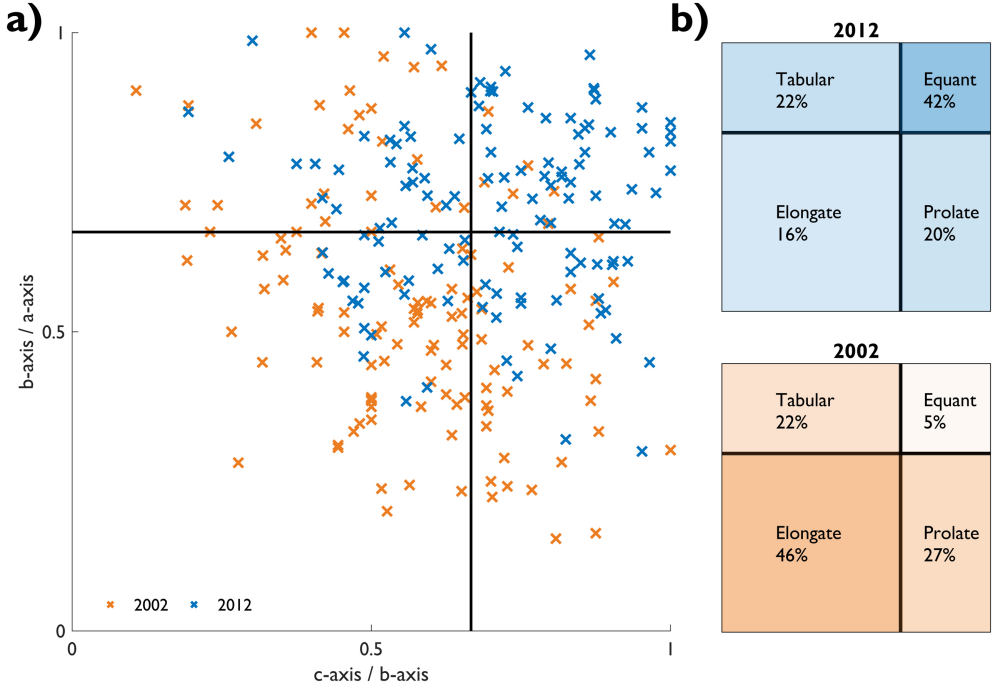
a)
b)
1
0.5
0
0
0.5
1
b-axis / a-axis
c-axis / b-axis
2002
2012
2012
Tabular
22%
Equant
42%
Elongate
16%
Prolate
20%
2002
Tabular
22%
Equant
5%
Elongate
46%
Prolate
27%

Figure 6

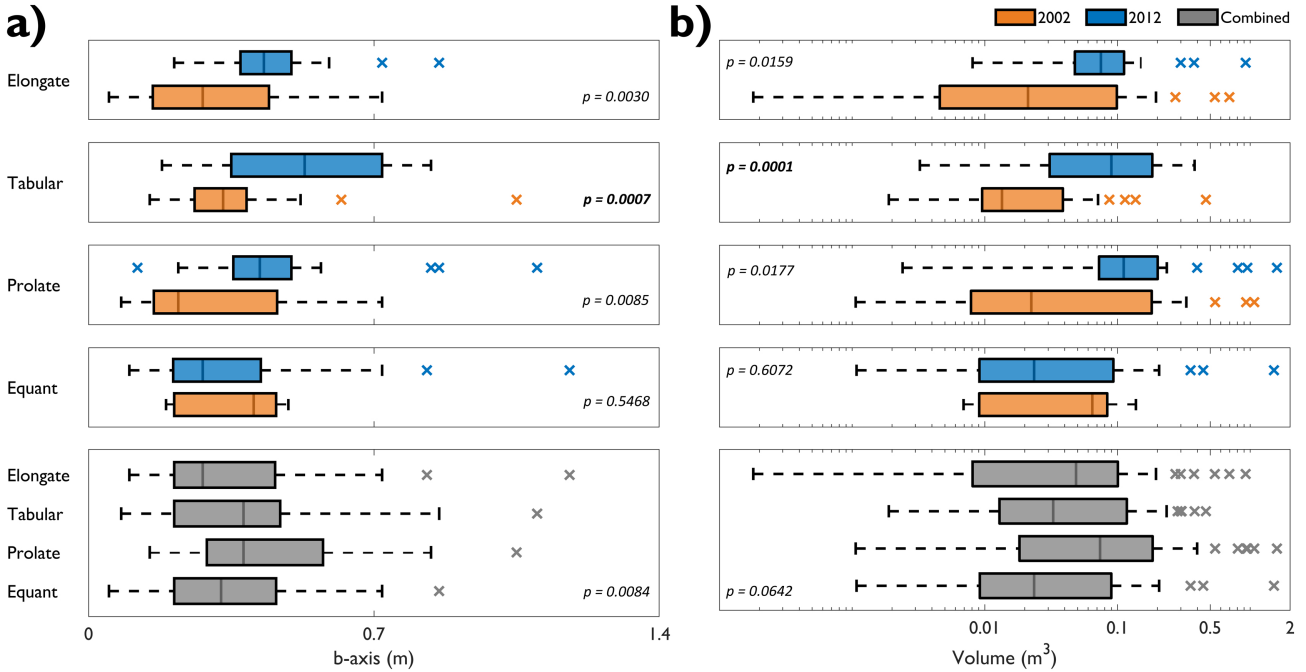
a)
b)
2002
2012
Combined
Elongate
Tabular
Prolate
Equant
Elongate
Tabular
Prolate
Equant
p = 0.0030
p = 0.0007
p = 0.0085
p = 0.5468
p = 0.0084
p = 0.0159
p = 0.0001
p = 0.0177
p = 0.6072
p = 0.0642
0
0.7
1.4
b-axis (m)
0.01
0.1
0.5
2
Volume (m3)

Figure 7

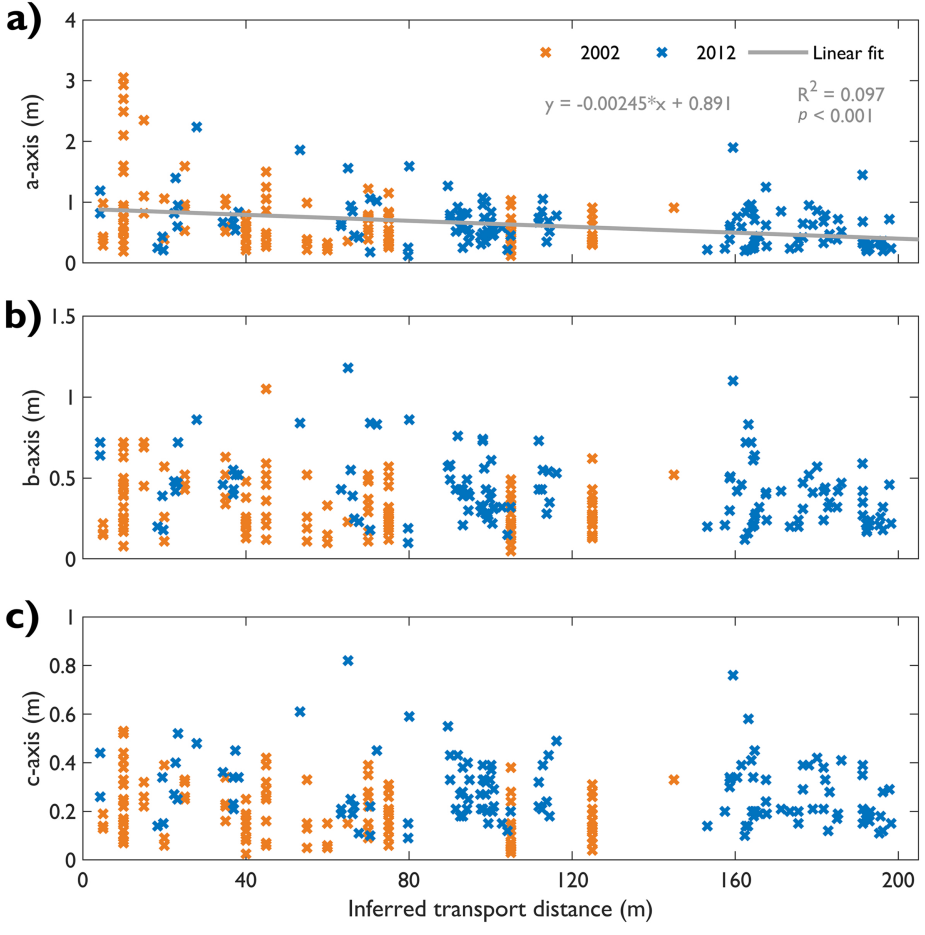
a)
b)
c)
2002
2012
Linear fit
y = -0.00245*x + 0.891
R2 = 0.097
p < 0.001
a-axis (m)
b-axis (m)
c-axis (m)
Inferred transport distance (m)
0
40
80
120
160
200

Figure 8

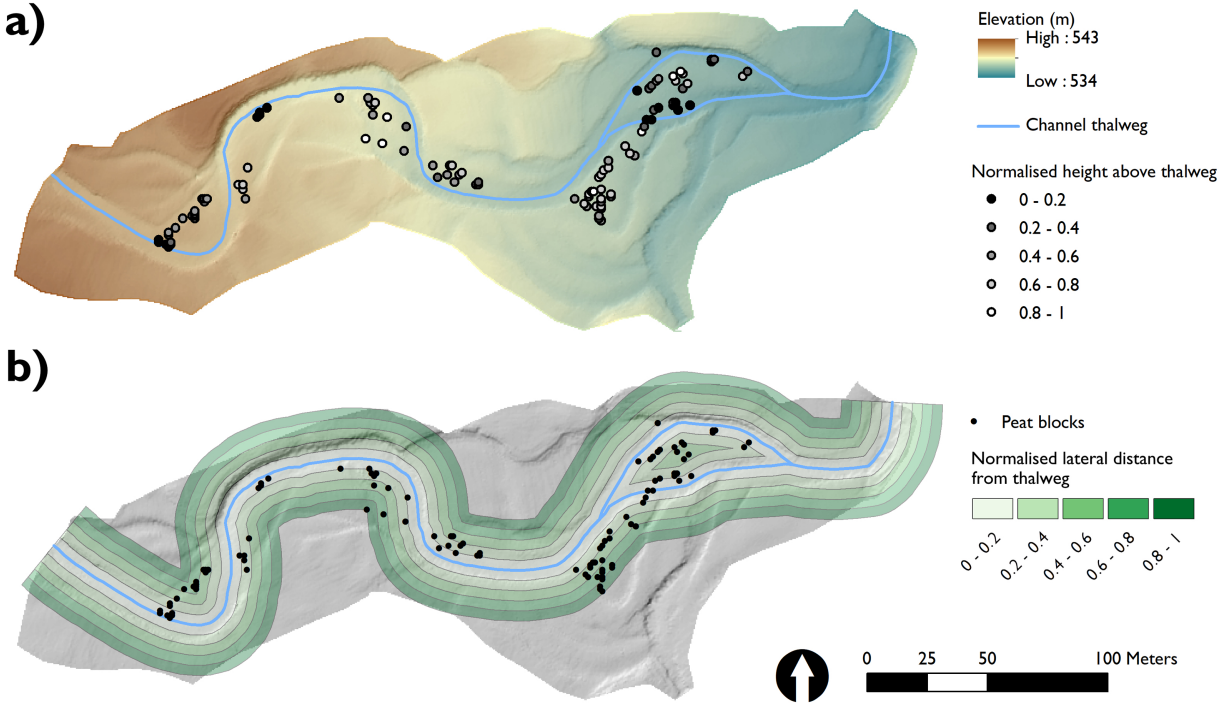
a)
Elevation (m)
High : 543
Low : 534
Channel thalweg
Normalised height above thalweg
0 - 0.2
0.2 - 0.4
0.4 - 0.6
0.6 - 0.8
0.8 - 1
b)
Peat blocks
Normalised lateral distance from thalweg
0 - 0.2
0.2 - 0.4
0.4 - 0.6
0.6 - 0.8
0.8 - 1
0
25
50
100 Meters

Figure 9

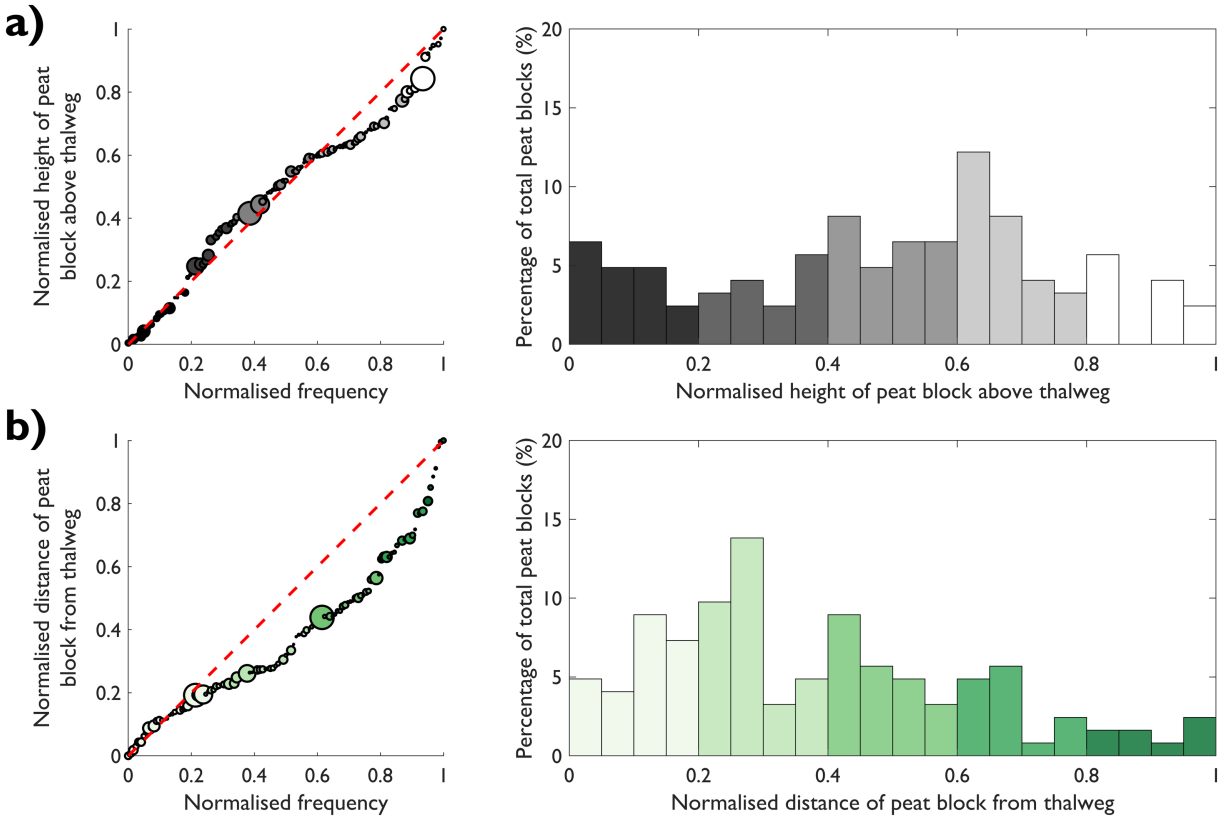
a)
Normalised height of peat block above thalweg
Normalised frequency
Percentage of total peat blocks (%)
Normalised height of peat block above thalweg
b)
Normalised distance of peat block from thalweg
Normalised frequency
Percentage of total peat blocks (%)
Normalised distance of peat block from thalweg

Figure 10

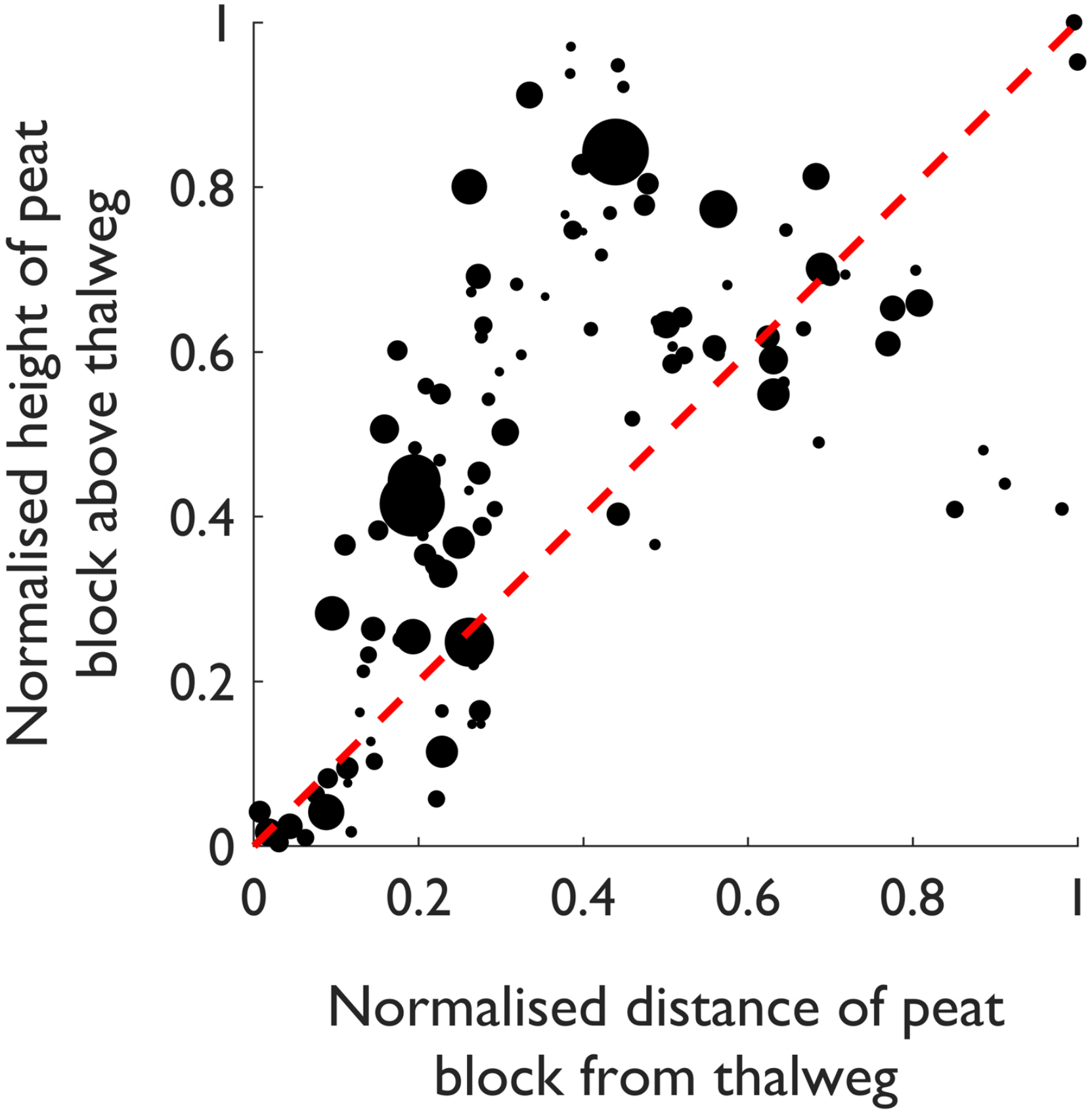
Normalised height of peat block above thalweg
0
0.2
0.4
0.6
0.8
1
0
0.2
0.4
0.6
0.8
1
Normalised distance of peat block from thalweg

Figure 11